

Post-T Tauri Stars in the Nearest OB Association

Eric E. Mamajek, Michael R. Meyer, & James Liebert

Steward Observatory, Dept. of Astronomy, University of Arizona, 933 N. Cherry Ave., Tucson, AZ 85721
eem@as.arizona.edu

ABSTRACT

We present results of a spectroscopic survey of X-ray- and proper motion-selected samples of late-type stars in the Lower Centaurus-Crux (LCC) and Upper Centaurus-Lupus (UCL) subgroups of the nearest OB association: Scorpius-Centaurus. The primary goals of the survey are to determine the star-formation history of the OB subgroups, and to assess the frequency of accreting stars in a sample dominated by “post-T Tauri” pre-main sequence (pre-MS) stars. We investigate two samples: (1) proper motion candidates from the ACT and TRC astrometric catalogs (Hoogerwerf 2000) with X-ray counterparts in the *ROSAT* All-Sky Survey (RASS) Bright Source Catalog, and (2) G and K-type stars in the *Hipparcos* catalog found to be candidate members by de Zeeuw et al. (1999). We obtained optical spectra of 130 candidates with the Siding Springs 2.3-m dual-beam spectrograph. Pre-MS stars were identified by (1) strong Li $\lambda 6707$ absorption, (2) subgiant surface gravities, (3) proper motions consistent with Sco-Cen membership, and (4) HR diagram positions consistent with being pre-MS. We find 93% of the RASS-ACT/TRC stars to be probable pre-MS members, compared to 73% of the *Hipparcos* candidates. We demonstrate that measuring the gravity-sensitive band-ratio of Sr II $\lambda 4077$ to Fe I $\lambda 4071$ is a valuable means of discriminating pre-MS and zero-age main sequence (ZAMS) stars. Using secular parallaxes, and *Hipparcos*, Tycho-2, and 2MASS photometry, we construct an HR diagram. Depending on the choice of published evolutionary tracks, we find the mean ages of the pre-MS populations to range between 17-23 Myr for LCC, and 15-22 Myr for UCL. Taking into account observational errors, it appears that 95% of the low-mass star-formation in each subgroup must have occurred in less than 8 Myr (LCC) and 12 Myr (UCL). Using the Bertelli et al. (1994) tracks, we find main sequence turn-off ages for *Hipparcos* B-type members to be 16 ± 1 Myr for LCC and 17 ± 1 Myr for UCL. Contrary to previous findings, it appears that LCC is coeval with, or slightly older than, UCL. The secular parallaxes of the Sco-Cen pre-MS stars yield distances of 85-215 pc, with 12 of the LCC members lying within 100 pc of the Sun. Only 1 out of 110 ($0.9^{+2.1\%}_{-0.8\%}$; 1σ) pre-MS solar-type stars in the sample with ages of 13 ± 1 (s.e.) ± 6 (1σ) Myr and masses of 1.3 ± 0.2 (1σ) M_\odot shows both enhanced H α emission and a K-band excess indicative of accretion from a truncated circumstellar disk: the nearby ($d \simeq 86$ pc) classical T Tauri star PDS 66.

Subject headings: Galaxy : open clusters and associations: individual (Sco OB2, Lower Centaurus-Crux, Upper Centaurus-Lupus) — stars: activity — stars: formation — stars: kinematics — stars: pre-main sequence — X-rays: stars

1. Introduction

Post-T Tauri stars (PTTSs) are low-mass, pre-main sequence (pre-MS) stars with properties intermediate between T Tauri stars found in molecular clouds (both “classical” with evidence for ac-

cretion from a circumstellar disk and “weak-lined” lacking such evidence; CTTSSs & WTTSSs; ages $<$ few Myr) and zero-age main sequence stars (ZAMS; ages $>$ 30-100 Myr). Although strict observational criteria do not exist for classifying PTTSs as such, a working definition is a low-

mass star ($<2 M_{\odot}$) that is Li-rich compared to stars in ZAMS open clusters such as the \sim 120 Myr-old Pleiades, and whose theoretical H-R position ($\log T_{\text{eff}}$ and $\log L/L_{\odot}$) is above the main sequence (Herbig 1978; Jensen 2001). Since these criteria also apply to CTTSs and WTTSs, one could argue that in addition, PTTSs should be located in regions devoid of nearby molecular gas or nebulosity. Classifying PTTSs by these criteria has complications: (1) few young field stars not associated with well-studied molecular clouds currently have accurately measured distances (hence known luminosities), (2) unresolved binarity can make stars with known distances appear more luminous, and thus younger, and (3) there is a dispersion in observed Li abundances among stars with the same masses and ages in coeval open clusters. Pre-main sequence stars exhibit considerable chromospheric ($\text{H}\alpha$, Ca H & K) and coronal X-ray emission. Only a few PTTS candidates were known before the *Einstein* and *ROSAT* X-ray missions, and X-ray surveys have become the primary means of identifying these pre-MS stars.

Investigations of pre-main sequence evolution have been hampered by a lack of large samples of well-characterized PTTSs. This deficit has impacted studies of pre-MS angular momentum evolution (e.g. Rebull et al. 2001; Bouvier et al. 1997), stellar multiplicity (e.g. Köhler et al. 2000), and circumstellar disk evolution (e.g. Spangler et al. 2001; Haisch, Lada, & Lada 2001). The nearest post-T Tauri stars also provide optimal targets for young exoplanet and brown dwarf searches (e.g. Lowrance et al. 2000). These objects are much more luminous early in their evolution, and the closest targets enable characterization of the smallest orbital radii. With a post-T Tauri population in a nearby OB association, we can address basic questions such as: How long does star-formation persist in a giant molecular cloud? What is the duration of the accretion phase for young solar-type stars?

Identifying a bona fide PTTS sample can be accomplished by searching for low-mass members of nearby fossil OB associations. The Sco-Cen OB complex (Sco OB2) is the nearest OB association to the Sun (mean subgroup distances range from 118-145 pc; de Zeeuw et al. (1999), hereafter dZ99), and covers roughly 2000 square degrees (\sim 5%) of the sky. The complex is comprised of

three kinematic subgroups (Blaauw 1946) with nuclear ages ranging from 5 to 15 Myr, a molecular cloud currently undergoing star-formation (the ρ Oph complex, Wilking, Lada, & Young 1989; Blaauw 1991; de Geus 1992), and perhaps several smaller cloud complexes in the vicinity (e.g. the Lupus, Corona Australis, Chamaeleon, Musca, and Coalsack clouds). The three subgroups are Upper Scorpius (US; age 5-6 Myr), Upper Centaurus-Lupus (UCL; age 14-15 Myr), and Lower Centaurus-Crux (LCC; age 11-12 Myr de Geus et al. 1989). US has been studied extensively in recent years (e.g. Preibisch & Zinnecker 1999, and references therein), however UCL and LCC have received relatively little attention.

In this work, we investigate the low-mass ($<2 M_{\odot}$) membership of the two oldest Sco-Cen OB subgroups (LCC and UCL) utilizing recently available astrometric catalogs (*Hipparcos*, Astrographic Catalog-Tycho (ACT), Tycho Reference Catalog (TRC), and *Tycho-2*), the 2 Micron All Sky Survey (2MASS), and the *ROSAT* All-Sky Survey (RASS). We conduct a spectroscopic survey of two samples: (1) an X-ray-selected sample of late-type stars from the kinematic candidate membership lists of Hoogerwerf (2000), and (2) the G-K type *Hipparcos* members of the OB subgroups from dZ99. In §2, we discuss the procedure for selecting candidate pre-MS stars from both samples, and §3 discusses the observations and assembled database. §4 describes the data analysis and characterization of our stellar sample, and §5 discusses the selection of pre-MS stars, sample contamination, and completeness. §6 describes how we construct an H-R diagram for the subgroups, and §7 presents results regarding the ages of the subgroups, their age spreads, and the frequency of accretion disks around pre-MS stars. §8 discusses the star-formation history of LCC and UCL, and §9 summarizes the findings of our survey.

2. Selection of Candidate Pre-MS Stars

2.1. The *Hipparcos* Sample

DZ99 lists *Hipparcos* Sco-Cen members that were selected using *both* de Bruijne's (1999a) refurbished convergent point method and Hoogerwerf & Aguilar's spaghetti method (1999). Their membership lists contained 31 G-K stars in UCL

and 21 G-K stars in LCC (their Table C1). Most of these bright stars have been classified in the Michigan Spectral Survey (e.g. Houk & Cowley 1975), however SIMBAD¹ reveals that most have been studied no further. We limit the survey to the 30 G-K candidates with Michigan luminosity classes IV or V (see Table 1). Stars with borderline F/G Michigan types were not observed. HIP 63962 and 73777 met the criteria, but were not observed. DZ99 estimated the contamination by G-K-type interlopers of all luminosity classes to be 32% for LCC and 24% for UCL. Of these 31 stars, 17 also have RASS-BSC X-ray counterparts within 40''.

2.2. The RASS-ACT/TRC Sample

To identify lower-mass members of an OB association, one can search for stars whose proper motions are similar to those of high-mass members. The high-mass membership and moving group solution for each OB subgroup were determined by dZ99 and de Bruijne (1999b). Thousands of faint stars in the ACT and TRC astrometric catalogs² were identified by Hoogerwerf (2000) as candidate low-mass LCC and UCL members. A high degree of contamination from interlopers is expected due to the similarity of the space motions of the subgroups to that of the Local Standard of Rest, compounded by the low galactic latitude of the subgroups. The selection of ACT/TRC candidate members is described in detail in §4 of Hoogerwerf (2000).

The Hoogerwerf ACT/TRC membership lists for LCC and UCL were slightly modified, and filtered, to produce the final target list. First, we requested from R. Hoogerwerf (personal communication) candidate membership lists with different color-magnitude constraints from that described in Hoogerwerf (2000). The new color-magnitude selection box is essentially a polygon defined by the Schmidt-Kaler (1982) empirical zero-age main sequence ($B - V$ vs. M_V) at the

¹<http://simbad.u-strasbg.fr/Simbad>

²The ACT (Urban et al. 1998) and TRC catalogs (Høg et al. 1998) were used for target selection for this project in 1999, however we use the photometry and astrometry from the Tycho-2 catalog (available in 2000; Høg et al. 2000a,b) in the data analysis. The Tycho-2 catalog was a joint USNO/Copenhagen project, and its data supercede the contents of the ACT and TRC catalogs.

mean distance for each subgroup (dZ99), where we take all stars $\Delta M_V = 3$ mag above and $\Delta M_V = 1$ mag below the ZAMS line. Hoogerwerf originally selected only those stars within $\Delta M_V = 1.5$ mag above the ZAMS, however this could inadvertently omit younger members or binaries. The selection box contained 1353 ACT and TRC stars in LCC, and 1874 stars in UCL. In order to target low-mass solar-type stars with G-K spectral types, we retained only those stars with Johnson $B - V \geq 0.58$ mag (the unreddened color of G0 dwarfs; Drilling & Landolt 2000). No red $B - V$ limit was imposed. After the color-magnitude selection, we retained only those stars which were identified as kinematic members in *both* the ACT and TRC astrometric catalogs. This final color-selection of the ACT/TRC lists resulted in 785 UCL candidates and 679 LCC candidates.

In order to further filter the target list, we selected only those ACT/TRC candidates which had *ROSAT* All-Sky Survey Bright Source Catalog (RASS-BSC) X-ray counterparts. Voges et al. (1999) cross-referenced the RASS-BSC with the Tycho catalog and found that 68% of the optical-X-ray correlations were within 13'', and 90% of the correlations were within 25''. In plotting a histogram of the separation distance between RASS-BSC X-ray sources and ACT/TRC stars, we independently find 40'' to be an optimal search radius. No constraints on X-ray hardness ratio were imposed in the target selection. In order to calculate X-ray luminosities, we assume the X-ray energy conversion factor for the *ROSAT* PSPC detector from Fleming et al. (1995). The linearity of this X-ray efficiency relation spans the temperature range of stellar coronae from inactive subdwarf stars to extremely active RS CVns and T Tauri stars. Unsurprisingly, the kinematic selection of ACT/TRC stars also selected many of the same stars as in the *Hipparcos* sample (HIP 57524, 59854, 62445, 65423, 66001, 66941, 67522, 75924, 76472, 77135, 77524, 77656, 80636). These stars are retained in the *Hipparcos* sample (Table 1), and omitted from the RASS-ACT/TRC list (Table 2). The final target list of 96 RASS-ACT/TRC stars (40 LCC, 56 UCL) is given in Table 2.

3. Observations

Blue and red optical spectra of the pre-MS candidates were taken simultaneously with the Dual-Beam Spectrograph (DBS) on the Siding Springs 2.3-m telescope on the nights of 20-24 April 2000. The DBS instrument is detailed in Rodgers, Conroy, & Bloxham (1988). Using a 2" wide slit, we used the B600 1/mm grating in first order on the blue channel, yielding 2.8Å FWHM resolution from 3838–5423Å. The red channel observations were done with the R1200 1/mm grating in first order, yielding 1.3Å FWHM resolution over 6205–7157Å. The five nights of bright time were predominantly clear to partly cloudy. Signal-to-noise ratios of \sim 50–200 per resolution element were typically reached with integration times of 120–720 s. Flat-fields and bias-frames were observed at the beginning and end of each night. NeAr λ -calibration arcs and spectrophotometric standards were observed every few hours. The spectra were reduced using standard IRAF routines. In order to remove low-order chromatic effects from the band-ratio measurements, we spectrophotometrically calibrated all of the target spectra using 2 standard stars from Hamuy et al. (1994). A total of 118 program stars (§2.1 and §2.2) and 20 MK spectral standards (§4.1.1) were observed. The major stellar absorption features of one of the single standard G stars were shifted to a zero-velocity wavelength scale. The spectra of all of the stars were then cross-correlated against this standard star using the IRAF task *fxcor*, and then shifted to the common, rest-frame wavelength scale. This was done to ensure proper identification of weak lines, as well as to make sure that the band-ratio measurements were sampling the same spectral range in each stellar spectrum.

4. Analysis of Spectra

4.1. Spectral Types and Luminosity Classification

4.1.1. Standard Stars

We observed 20 spectral standards including dwarfs and subgiants (luminosity classes IV and V) and a few giants (III). A summary of their properties is listed in Table 3. To permit quantitative examination of trends in the strengths of spectral features, as well as interpolation between

spectral types, we adopt the numerical subtype scaling of Keenan (1984; i.e. here listed as “SpT”, where G0 = 30, G2 = 31, K0 = 34, etc.). All of the standard stars are classified on the MK system by Keenan & McNeil (1989), except for HR 7061 (Garcia 1989). Table 3 also lists their spectral types as given in the Michigan Spectral Survey atlases of N. Houk (e.g. 1978). The sample standard deviation of a linear fit between the Keenan and Houk spectral types for dwarfs and subgiants, on Keenan’s subtype scale, is $\sigma(\text{SpT}) = 0.6$ subtypes. The ~ 0.6 subtype uncertainty probably represents the best that can be done using visual spectral types determined by different authors.

The adopted spectral types are those of Keenan & McNeil’s, however the luminosity classification was verified (and some times changed) by virtue of (1) position of the stars on a color-magnitude diagram based on *Hipparcos* data, (2) position in a temperature vs. Sr II $\lambda 4077/\text{Fe I } \lambda 4071$ ratio diagram (see §4.1.3, Fig. 1), and (3) published $\log g$ estimates. Although changing the classification of some standards may appear imprudent, the H-R diagram positions, Sr/Fe line ratio, and derived $\log g$ values (Cayrel de Strobel et al. 2001) are all consistent with our new adopted luminosity classes³. In every case the difference was only half of a luminosity class, and only 5/20 of the stars were changed. Notes on the revised luminosity classifications are given in Appendix B.

4.1.2. Visual Classification

The blue spectrum of each star was assigned a spectral type visually by E.M. through comparison with the standards in Table 3. In order to distinguish subtypes, we focused on several features such as the G band ($\lambda 4310$), Ca I $\lambda 4227$, Cr I $\lambda 4254$ and nearby Fe lines, and the Mg b lines $\lambda 5167$, $\lambda 5173$, $\lambda 5184$. Balmer lines were ignored due to possible chromospheric emission. After making an initial guess through comparison with a wide range of spectral types, a final visual spectral type was assigned through comparison to standards within ± 2 subtypes of the initial guess.

To test the accuracy of our visual classification, we compared our spectral types to those of qual-

³ *Hipparcos* data also led Keenan & Barnbaum (1999) to revise the luminosity classes of a few giant star standards at the half luminosity class level.

ity 1 or 2 in the Michigan Spectral Survey. The average difference is not significant: -0.4 ± 0.6 (1σ sample standard deviation) subtypes (on Keenan's scale). The 12 *Hipparcos* stars were later visually typed a second time. Between the two estimates for each star, we estimate that the 1σ uncertainty in our visual spectral types is 0.6 subtypes. This is comparable to the dispersion between the Keenan and Houk spectral types for the standards themselves.

4.1.3. Quantitative Spectral Type Estimation

A two-dimensional quantitative spectral type (subtype plus luminosity class) can be estimated using integrated fluxes over narrow bands sensitive to temperature and surface gravity. We tested various ratios defined by Malyuto & Schmidt-Kaler (1997) and Rose (1984) for this purpose, as well as from Gray's spectral atlas (2000). In testing band-ratios as temperature indicators for our standards, we noticed that some had slight surface gravity dependencies. A surface gravity dependence in our temperature indicators could systematically affect our T_{eff} estimates. We first discuss our surface gravity indicator and then define our temperature estimators using only subgiant and dwarf standards, thus mitigating the effects of surface gravity.

The most widely used surface gravity diagnostic for G and K stars is the ratio between Sr II $\lambda 4077$ and nearby Fe lines (e.g. Keenan & McNeil 1976; Gray 2000). In thin and thick disk dwarfs, the abundance ratio [Sr/Fe] is within ~ 0.1 dex of solar for most stars (Mashonkina & Gehren 2001). A quantitative surface gravity (luminosity class) indicator was established by Rose (1984) from low-resolution spectra using the maximum absorption line depth for Sr II $\lambda 4077$ and the average for the atomic Fe $\lambda 4045$ and $\lambda 4063$ lines. We measure the fluxes in 3 Å bands centered on the Sr II $\lambda 4077$ line and the Fe I $\lambda 4071$ line. Ratios between the $\lambda 4077$ line and the other nearby Fe lines ($\lambda 4045$, $\lambda 4063$) did not distinguish subgiants and giants.

For a temperature estimator, we adopted Index 6 of Malyuto & Schmidt-Kaler (1997) ($\lambda\lambda 5125$ - $5245/\lambda\lambda 5245$ - 5290) hereafter referred to as "MI6". The temperature sensitivity of this indicator largely reflects differing amounts of line-blanketing in these two wavelength regimes – mainly by the Mg b lines ($\lambda 5167$, $\lambda 5173$, and $\lambda 5184$), and many

Fe lines (e.g. Fe I $\lambda 5270$). Although the Mg b lines are somewhat surface gravity sensitive, within the $\log g$ and T_{eff} regime of our standards and program stars, the temperature sensitivity is dominant. The difference in central wavelength between the two bandpasses is only 82 Å, and the effects of reddening are negligible (Mathis 1990). For a temperature indicator, we fit a low-order polynomial to MI6 vs. SpT for the dwarf and subgiant standard stars (see Appendix C) which has a 1σ sample standard deviation of 0.6 subtypes.

Fig. 1 plots the temperature-sensitive MI6 index versus our surface gravity discriminant (Sr II $\lambda 4077$ /Fe I $\lambda 4071$). The dwarf standards form a very narrow sequence in Fig. 1, *confirming the lack of cosmic scatter in [Sr/Fe] values among field stars and the insensitivity of log g to spectral type for G-K dwarfs*. The polynomial fit to the dwarf data is given in Appendix C. There is a gap between the dwarf and subgiant loci between ~ 1 - 2.5σ (sample standard deviation) of the dwarf locus polynomial, and we set the subgiant/dwarf separation at 2σ . We classify stars within 2σ of the solid dwarf line in Fig. 1 as dwarfs (4 of 96 RASS-ACT/TRC stars, 4 of 20 HIP stars), and three stars near the giant locus (TYC 8992-605-1, HIP 68726, and HIP 74501) as giants. We classify the rest as subgiants.

Gray (2000) suggests Y II $\lambda 4376$ /Fe I $\lambda 4383$ as a surface gravity indicator for late-G stars using low-resolution spectra. From the solar spectral atlas of Wallace, Hinkle, & Livingston (1998), it appears that Gray's low-resolution Y II $\lambda 4376$ feature is actually a blend of several lines of nearly equal strength. In order to test the properties of this band-ratio, we measure the flux in 3 Å windows centered on wavelengths 4383.6 Å and 4374.5 Å. Plotting this ratio against spectral type for the standard stars showed a very tight locus for the dwarfs, however luminosity classes IV-V, IV, and III were indistinguishable from the dwarfs and each other. We found this ratio unsuitable for the purposes of luminosity classification of our targets, but we find it to be an excellent temperature estimator for FGK dwarfs, subgiants, and giants. Among the 20 standards, the measurement of the $\lambda 4374/\lambda 4383$ band-ratio vs. spectral type gives a tight correlation (sample standard deviation $1\sigma = 0.6$ subtypes). We adopt the $\lambda 4374/\lambda 4383$ band ratio as our third, independent estimator of spec-

tral type (polynomial fit is given in Appendix C).

4.1.4. Final Spectral Types

The three temperature-type estimates agree well for the majority of the program stars. The mean difference between the MI6 and visual spectral types is 0.7 subtypes. The mean difference between the $\lambda 4374/\lambda 4383$ band-ratio types and the visual types is 0.6 subtypes. We calculate a mean spectral type and standard error of the mean using the three classifications. The mean is unweighted since all three relations appeared to have 1σ sample standard deviations of ≈ 0.6 subtypes in their accuracy. The average standard error of the mean is 0.5 subtypes. We believe that using multiple techniques mitigates the effects that rapid rotation, binarity, etc. can introduce into visual classification alone. The spectral types are listed in Tables 6, 5 and 7.

4.2. Additional Spectroscopic Diagnostics

4.2.1. Chromospheric $H\alpha$ Emission

Medium-to-low resolution spectra of chromospherically active stars show the $H\alpha$ line to be partially filled-in, or even fully in emission. We measure the EW of the entire $H\alpha$ feature; our resolution is insufficient to separate the “core” chromospheric emission from the photospheric $H\alpha$ absorption line. A significant number of our stars show $H\alpha$ emission (19% of the RASS-ACT/TRC G-K type stars). We characterize our targets stars as chromospherically active or inactive through comparing the $H\alpha$ EW to that of standards of identical spectral type. Fig. 2 shows the EW($H\alpha$) data for our targets and standard stars. Stars more than 2σ above the dwarf/subgiant EW($H\alpha$) relation (a quadratic regression; see Appendix C) are considered to be active. The stars with $H\alpha$ in emission (negative EWs) have an “e” appended to their spectral types in Tables 6, 5 and 7. The $H\alpha$ EWs for each star are also listed in these tables.

4.2.2. $Li\ I\ \lambda 6707$ Equivalent Width

The presence of strong Li absorption in the spectra of late-type stars is a well-known diagnostic of stellar youth. Because of the extended timescale for significant Li depletion in stars of $\sim 1 M_\odot$, *strong Li absorption is necessary, but not sufficient indicator of pre-MS nature for G stars.*

However it is a powerful age discriminant when combined with our surface gravity indicator.

Many studies have shown that the equivalent width (EW) of $Li\ I\ \lambda 6707$ can be overestimated at low spectral resolution (e.g. Covino et al. 1997), especially for G-K stars. With a resolution of 1.3\AA , we consider our EWs to be approximate. The EWs were measured with Voigt profiles in the IRAF routine *splot*. The continuum level was estimated from nearby pseudo-continuum peaks. We subtract the contribution from the neighboring $Fe\ I\ \lambda 6707.4\text{\AA}$ feature using the prescription of Soderblom et al. (1993). In order to test the validity of our Li EWs, we divided several of our Li-rich targets by standard stars of the same spectral type. The ratioed spectra exhibit only a major absorption feature at $\lambda 6707$. The division also removes the effects of blending by Fe lines (assuming the same stars have similar EWs). The EWs of this feature in the divided spectra corresponded well with our previous measurements, however the uncertainties in the EW appear to be $\sim 20\text{--}50\text{ m\AA}$ (with the maximum value being for spectroscopic binaries).

Fig. 3 shows the $Li\ I\ \lambda 6707$ EWs for our RASS-ACT/TRC and *Hipparcos* targets, separated according to their luminosity class (§4.1.3). Effective temperatures (T_{eff}) come from the final spectral type (see §6.2). Most points lie above the $Li\ I\ \lambda 6707$ EWs that characterize young open clusters, plotted as low-order polynomial fits for the IC 2602 (30 Myr; Randich et al. 1997), Pleiades (70–125 Myr; Soderblom et al. 1993; Basri, Marcy, & Graham 1996), and M34 clusters (250 Myr; Jones et al. 1997). The comparison is not completely fair, however, since the cluster ZAMS stars will be roughly 10% less massive than the corresponding pre-MS stars. Even if most of our program stars were older ZAMS stars, they still would be Li-rich compared to stars in the well-studied open clusters. We select as “Li-rich” those stars above the solid line in Fig. 3. Considering the uncertainties in our EW(Li) measurements, and the lack of any other $\sim 10\text{--}20$ Myr-old pre-MS G-K-type stellar samples with which to compare, we are not compelled to subdivide our sample further. We will reserve a more detailed investigation of the Li abundances for a future high-resolution spectral study. For the present, we are content to have demonstrated that we have identified a popula-

tion which appears to be more Li-rich than ZAMS stars.

5. Defining the PTTS Sample

5.1. Membership Status

Our survey was designed to identify the pre-MS G and K-type stars in the Sco-Cen OB association. We classified the late-type stars according to their positions in Figs. 1, 2 and 3 (Table 4). We consider the 110 stars (85/96 RASS-ACT/TRC and 16/30 *Hipparcos*) classified as “Li-rich”, “subgiant”, and “active” as bona fide post-T Tauri stars (“pre-MS”). Li-rich stars with subgiant surface gravities and $H\alpha$ EWs similar to the standard field stars (i.e. “inactive”) are called “pre-MS?”. Only 3 of the RASS-ACT/TRC stars, and 6 of the HIP stars are classified as “pre-MS?”. The lone object with giant-like surface gravity in the RASS-ACT/TRC X-ray-selected sample (TYC 8992-605-1) is Li-rich, and we also classify it as a pre-MS PTTS. The 9 “pre-MS?” stars were included in our statistics concerning the star-formation history and disk-frequency of the sample (§7) for a total of 110 candidate lower-mass members of the LCC and UCL subgroups. All 13 stars selected in the RASS-ACT/TRC sample which overlaped with dZ99’s membership lists were found to be pre-MS candidates. Our RASS-ACT/TRC sample (including the 13 dZ99 stars also selected) yielded a pre-MS hit-rate of $(88+13)/(96+13) = 93\%$. Of the 30 dZ99 candidates we observed, 22/30 (73%) are classified as pre-MS or “pre-MS?”. The numbers of stars by membership class are listed in Table 4. Pre-MS stars in the *Hipparcos* sample are listed in Table 5, and those in the RASS-ACT/TRC sample are given in Table 6. Li-rich stars with dwarf-like surface gravity ($N = 5$) were considered young main sequence field stars (“ZAMS”), and are listed along with other interlopers in Table 7.

5.2. Sample Contamination

The primary contaminants one would expect from an X-ray- and proper motion-selected sample are X-ray-luminous ZAMS stars (ages ≈ 0.1 -1 Gyr). Field ZAMS stars could occupy the same region of UVW velocity space, and be selected in our study by virtue of their proper motions and X-ray emission. However, our selection of candidate

Sco-Cen members utilizes a surface gravity criterion which should minimize contamination. Even if our surface gravity indicator was in error, we claim ZAMS stars do not dominate our sample. Field ZAMS stars exhibit a large spread in Li EWs (especially for the late-G and early-K stars), however this is not observed in Fig. 3. The star just below the “Li-rich” line in Fig. 3 (TYC 7318-593-1; G9, $EW(Li) \simeq 150$ mÅ) happens to be the sole RASS-ACT/TRC star with inferred $\log g$ higher than that of the dwarf standards in Fig. 1. We consider TYC 7318-593-1 to be a field ZAMS star candidate due to its intermediate Li strength and high surface gravity.

We can rule out most of the pre-MS candidates being Li-rich *post-MS* stars. Based on the surveys of Li abundances in field subgiants by Randich et al. (1999) and Pallavicini et al. (1987), we do not expect to find any post-MS subgiants with $EW(\lambda 6707) > 100$ mÅ. Even if our measured EWs for the Li I $\lambda 6707$ line are over-estimated due to low spectral resolution, the overestimate would have to be greater than a factor of two to reconcile our sources with even the most Li-rich subgiants found in the Randich et al. survey. Our spectral analysis suggests that the majority of our sample stars are both Li-rich and above the main sequence (i.e. pre-MS).

Could some of our stars be *post-MS* chromospherically active binaries (CABs) or RS CVn systems? The light from an RS CVn system would be dominated by a rapidly rotating, evolved (subgiant) primary. Only six of our targets are Li-poor subgiants (HIP 63797, 81775, TYC 8293-92-1, 7833-1106-1, 7858-526-1, and 8285-847-1). The first three appear to be normal subgiants. TYC 7833-1106-1 is possibly a spectroscopic binary. TYC 7858-526-1 has a wide, broad $H\alpha$ absorption line. It appears to be a multiple late-F star (we classify it as F8.5; Houk (1982) classify it as F5), so the star could hide a cosmic Li abundance due to the increased ionization of Li I in F stars (and correspondingly lower $EW(Li)$). The system could be a legitimate member, but we exclude it from the pre-MS sample. The subgiant TYC 8285-847-1 (HIP 69781 = V636 Cen) is probably a CAB. It is a previously known grazing, eclipsing binary (e.g. Popper 1966) and its saturated X-ray emission argues for being a true CAB. Finally, the Li-rich star TYC 8992-605-1

(star #19; K0+III) is the only RASS-ACT/TRC star that appears in the giant regime of Fig. 1. The star is an obvious spectroscopic binary of nearly equal mass. We believe this star is probably a pre-MS binary, and include it in our “pre-MS?” sample. It appears that CABs are a negligible contaminant when using X-ray and kinematic selection in tandem with medium dispersion spectroscopy to identify pre-MS populations.

5.3. Sample Completeness

We can make a rough estimate how many stars our selection procedure should have detected by counting the number of massive Sco-Cen members in a certain mass range, and assuming an initial mass function. We assume a complete membership census within a limited mass range (the revised B-star *Hipparcos* membership from dZ99), and then extrapolate how many stars we should have seen in our survey. We produce a theoretical H-R diagram for the subgroups’ B stars (discussed at length in §7.2), and calculate masses from the evolutionary tracks of Bertelli et al. (1994) ($Z=0.02$). We choose $2.5 M_{\odot}$ as our lower mass boundary (roughly the lower limit for B stars), and adopt $13 M_{\odot}$ as the upper mass boundary (slightly higher than the highest inferred mass from the main sequence members). In this mass range, we count 32 LCC members and 56 UCL members. We use a Kroupa (2001) IMF to predict how many low-mass stars might belong to the OB subgroups. Down to the hydrogen-burning limit ($0.08 M_{\odot}$), a total population of 1200^{+200}_{-300} stars in LCC and 2200 ± 300 stars in UCL is predicted (Poisson errors)⁴. Between 1.1 - $1.4 M_{\odot}$, the mass range of a 15 Myr-old population that our survey can probe (see §7.1 and Fig. 6), the Kroupa IMF predicts a population of 29^{+6}_{-5} stars in LCC, and 51^{+8}_{-7} stars in UCL. In this mass range, our survey detects 36 pre-MS stars in LCC and 40 pre-MS stars in UCL. The number of observed pre-MS stars with 1.1 - $1.4 M_{\odot}$ corresponds to $+1.1\sigma$ and -1.6σ of the predicted number, for LCC and UCL respectively. This suggests that our survey is fairly complete for LCC, but we might be missing ~ 10 members with masses of 1.1 - $1.4 M_{\odot}$ in the more distant UCL subgroup if the subgroup mass

⁴For low-number statistical uncertainties, we use the 1σ values from Gehrels (1986) throughout.

function is consistent with the field star IMF. The missing members of the UCL OB subgroup could be X-ray faint ($L_X \leq 10^{30.2}$ erg s $^{-1}$) stars which we were capable of detecting in the closer LCC subgroup. The IMF extrapolation does suggest that we have likely found at least the majority of stars in this mass range in both OB subgroups (if not a complete census for LCC) and that our samples are representative of the total population.

6. The H-R Diagram

In order to investigate the star-formation history of the LCC and UCL OB subgroups, we convert our observational data (spectral types, photometry, distances) into estimates of temperature and luminosity. We then use theoretical evolutionary tracks to infer ages and masses for our stars.

6.1. Photometry

The primary sources of photometry for our sample of association member candidates are the Tycho-2 catalog (Høg et al. 2000a,b) and 2MASS working database. However, the Tycho and 2MASS bandpasses are non-standard, and must be converted to standard photometric systems to enable comparison with intrinsic colors of normal stars and the interstellar reddening vector. To convert the Tycho photometry to the Johnson system, we fit low-order polynomials to the data in Table 2 of Bessell (2000) (relations given in Appendix C). A caveat is that Bessell’s calibrations are for B-G dwarfs and K-M giants. The majority of our stars appear to be pre-MS G-K stars, whose intrinsic colors should more closely match those of dwarfs rather than giants. To convert the 2MASS JHK_s data to the system of Bessell & Brett (1988), we use the conversions of Carpenter (2001). The original optical and near-IR photometry for our target stars is given in Tables 2 and 1.

6.2. Temperature Scale

To fix stellar properties as a function of spectral type, we adopt relations (i.e. intrinsic colors, BCs) from Table A5 of Kenyon & Hartmann (1995). Previous studies have shown that colors and BCs as a function of T_{eff} are largely independent of surface gravity over the range of interest for this study (e.g. Bessell, Castelli, & Plez

1998). However, T_{eff} decreases with lower $\log g$ for FGK stars. After some investigation (see Appendix A), we decided to adopt the dwarf T_{eff} scale of Schmidt-Kaler (1982) (which Kenyon & Hartmann (1995) also use) with a -35 K offset to account for the effects of lower $\log g$ in our sample stars. The scatter in published dwarf T_{eff} scales is 60 K (1σ) among G stars, so while the shift is systematic, its magnitude is of the order of the uncertainties. The uncertainties in T_{eff} given in column 9 of Tables 5 and 6 include the uncertainty in spectral type and the scatter in published T_{eff} scales. The typical 1σ uncertainties in T_{eff} for the pre-MS stars is ≈ 100 K.

6.3. Secular Parallaxes

All of the stars in our sample have published proper motions, but only a few dozen have trigonometric parallaxes measured by *Hipparcos*. The stars are distributed over hundreds of square degrees of sky, and inhabit stellar associations which are tens of parsecs in depth. Adopting a standard distance for all of the stars in the association introduces unwanted scatter in the H-R diagram. With accurate proper motions available, we calculate individual distances to the pre-MS candidates using moving cluster or “secular” parallaxes (e.g. Smart 1968). We adopt the equations and formalism of de Bruijne (1999b), as well as his space motions and convergent points for the LCC and UCL OB subgroups. The uncertainties in the secular parallaxes are dominated by the uncertainties in the proper motion ($\sigma_\pi \propto \sigma_\mu$), but contain a term added in quadrature accounting for a projected 1 km s^{-1} internal velocity dispersion (see §4 of de Bruijne 1999b). The secular parallax is only meaningful if the star is indeed a member of the group. Our spectroscopic survey has confirmed that most of the candidate stars are legitimately pre-MS, and that they are most likely members of the OB subgroups. Secular parallaxes for older, interloper stars are meaningless and ignored. In Tables 5 and 6, we list the secular parallaxes and membership probabilities for the pre-MS stars in our survey. We calculate membership probabilities P_1 and P_3 (using formulae 4 and 6 from dZ99), which have assumed internal velocity dispersions of 1 km s^{-1} (de Bruijne 1999b) and 3 km s^{-1} (dZ99), respectively.

The robustness of our method can be illustrated

(Fig. 4) by comparing the secular parallaxes (π_{sec}) to the *Hipparcos* trigonometric parallaxes (π_{HIP}). The uncertainties are typically 1-2 mas for the *Hipparcos* parallaxes, and 0.5-1 mas for our secular parallax estimates. The secular and trigonometric parallaxes agree quite well for the few pre-MS stars in our sample for which *Hipparcos* measured the parallax. The secular parallaxes yield distance uncertainties of $\sim 5\text{-}15\%$ for most of the pre-MS stars.

6.4. Luminosities

With five-band photometry, a temperature / spectral type estimate, and a secular parallax, we calculate stellar luminosities for the pre-MS candidates. We adopt the absolute bolometric magnitude of the Sun ($M_{bol\odot} = 4.64$) from Schmidt-Kaler (1982). In order to compromise between the uncertainties in luminosity due to reddening, photometric uncertainties, and possible K-band excess, we calculate the M_{bol} using the dereddened 2MASS J magnitude. We estimate the visual extinction from a weighted mean of A_V estimates from the color excess in $B - V$ and $V - J$. We took the $E(B - V)$ formula from Drilling & Landolt (2000) and the value of $A_J/A_V (= 0.294)$ was taken from the near-IR extinction law of Mathis (1990) for a central wavelength $1.22 \mu\text{m}$. The reddening A_J typically ranged from 0 to 0.35 mag with formal uncertainties of ~ 0.1 mag. The typical uncertainty in $\log L/L_\odot$ for the pre-MS candidates is ≈ 0.08 dex. With the luminosities and X-ray fluxes from the RASS BSC catalog (Voges et al. 1999), we calculate the ratio of X-ray/bolometric radiation for the stars with X-ray counterparts. The derived values of $\log(L_X/L_{bol})$ are in the range of $10^{-2.8} - 10^{-3.8}$, indicating coronal X-ray emission elevated above most ZAMS G-type stars (e.g. Pleiads; Stauffer et al. 1994).

6.5. Evolutionary Tracks

In order to infer theoretical masses and ages from our pre-MS candidates, we use the evolutionary tracks from D’Antona & Mazzitelli (1997) (DM97; $Z = 0.02$, $x_D = 2 \times 10^{-5}$), Siess, Dufour, & Forestini (2000) (SDF00; $Z = 0.02$), and Palla & Stahler (2001) (PS01). Ages and masses for a given $\log T_{eff}$ and $\log L/L_\odot$ were calculated using an interpolation algorithm. Given the mean observational errors ($\sigma(\log T_{eff}, \log L/L_\odot)$

$= 0.007$, 0.078 dex for LCC Pre-MS stars, and $\sigma(\log T_{eff}, \log L/L_{\odot}) = 0.009$, 0.084 dex among UCL Pre-MS stars), we estimate the isochronal age uncertainties for an individual star to be approximately 4 , 5 , 7 Myr (DM97, PS01, SDF00) in LCC, and 4 , 5 , 5 Myr (DM97, PS01, SDF00) in UCL, as illustrated in Fig. 5. The uncertainties in the interpolated masses are $0.1 M_{\odot}$ for all three sets of tracks. Fig. 6 shows the H-R diagram for the pre-MS candidates overlayed with the evolutionary tracks of DM97.

7. Results

The ages of the low-mass population of LCC and UCL have not been estimated before, though de Geus et al. (1989) and de Zeeuw & Brand (1985) give main sequence turn-off ages. In §7.1 we estimate the pre-MS ages for the two subgroups, and put an upper limit on the intrinsic age spread. In §7.2 we calculate new turn-off ages for the subgroups using early B stars from the revised *Hipparcos* membership lists of dZ99.

7.1. Pre-MS Ages and Age Spread

The H-R diagram for our “pre-MS” and “pre-MS?” stars is shown in Fig. 6, overlayed with the evolutionary tracks of D’Antona & Mazzitelli (1997). The temperatures and luminosities of the pre-MS stars are given in Columns 9 and 10 of Tables 6 and 5, along with their inferred masses and ages (columns 15 through 17). One notices immediately that the bulk of isochronal ages are in the range of ~ 10 - 20 Myr. The age range is nearly identical for both groups. To assess the effects of our magnitude limit in biasing our mean age estimates, in Fig. 7 we plot the mean pre-MS age (with standard errors of the mean) for the pre-MS subgroup samples as a function of minimum $\log T_{eff}$ cut-off. The magnitude bias of our survey is clearly apparent: the mean age systematically decreases when stars with $\log T_{eff} < 3.73$ are included in the calculation. In calculating the pre-MS ages of the OB subgroups, we explicitly omit the pre-MS stars with $\log T_{eff} < 3.73$ (30% of our sample). This temperature threshold intersects our magnitude limits at ages of ~ 25 Myr for stars of $1 M_{\odot}$ on the DM97 tracks. That the lines in Fig. 7 are nearly flat for $\log T_{eff} > 3.73$, suggests that (detectable) stars with ages of > 25 Myr

are not a significant component of either subgroup (also see discussion in §8.1).

Fig. 8 displays histograms of the isochronal ages for the pre-MS stars in the LCC and UCL subgroups derived using DM97 and SDF00 evolutionary tracks. These tracks represent the extrema in age estimates for our sample (DM97 is youngest, SDF00 is oldest). The 1σ age dispersion among the unbiased samples ($\log T_{eff} > 3.73$) is 5-9 Myr for both groups. If we remove the known spectroscopic binaries (see notes in Tables 6 and 5), the age dispersions are 4-8 Myr. Because there may be additional unresolved binaries, this *observed* age spread places an upper limit on the *intrinsic* age spread. As illustrated in Fig. 5, the individual H-R diagram positions of the pre-MS samples have $\log T_{eff}$ and $\log L/L_{\odot}$ errors which fold onto the evolutionary tracks with age uncertainties of 4-7 Myr. From this analysis, we conclude that the *intrinsic* 1σ age dispersions in each subgroup must be less than 2-8 Myr (i.e. $\sim 2/3$ rds of the star-formation took place in < 4 - 16 Myr). Using the DM97 pre-MS ages, which agree best with the turn-off age estimates (§7.2), we find intrinsic 1σ age dispersions of 2 Myr (LCC) and 3 Myr (UCL). *This implies that 68% of the low-mass star-formation took place within < 4 - 6 Myr, and 95% within < 8 - 12 Myr in the OB subgroups.* Our observational uncertainties and lack of knowledge about the unseen binarity of the pre-MS sample stars do not allow us to constrain the age spread more precisely than this. The mean age estimates for our unbiased pre-MS samples ($\log T_{eff} > 3.73$, SBs removed) are shown in Table 8. Counter to previous studies, we find that LCC is slightly older than UCL by 1-2 Myr (at $1-3\sigma$ significance), independent of which evolutionary tracks we use. From Fig. 8, we also conclude that star-formation ceased approximately ~ 5 - 10 Myr ago in the subgroups.

7.2. Turn-off Ages

De Geus et al. (1989) published the most recent age estimates for the LCC and UCL groups, but in light of the new *Hipparcos* distances and subgroup membership lists, we feel it is worthwhile reevaluating the subgroups’ turn-off ages. We construct a theoretical H-R diagram for the B-type subgroup members of UCL and LCC listed both in Table C1 of dZ99 and Tables A2 and A3

of de Bruijne (1999b). Several of the “classical”⁵ members rejected as members by *Hipparcos* from dZ99 are included as well. For input data, we use the following databases in order of availability: (1) $ubvy\beta$ photometry from the database of Hauck & Mermilliod (1997), (2) UBV photometry from Slawson, Hill, & Landstreet (1992), and (3) UBV photometry from SIMBAD. For distances we use the secular parallaxes (π_{sec}) given in column 4 of Tables A2 and A3 of de Bruijne (1999b) when available, or the *Hipparcos* parallaxes (π_{HIP}). We deredden the stars with $ubvy\beta$ photometry to the B-star sequence of Crawford (1978) using the prescription of Shobbrook (1983). For stars with Stromgren photometry, we calculate T_{eff} using the temperature relation of Napiwotzki, Schönberner, & Wenske (1993). If no $ubvy\beta$ photometry was available, we use UBV photometry to calculate the reddening-free index Q (Crawford & Mandewala 1976) to infer the star’s unreddened color. A polynomial fit to Table 15.7 from Drilling & Landolt (2000) is used to calculate T_{eff} as a function of $(B - V)_0$. The BC versus T_{eff} relation of Balona (1994) is used for all stars. We linearly interpolate between the isochrones from Bertelli et al. (1994) ($Y = 0.28$, $Z = 0.02$, convective overshoot) to infer ages for the subgroup B stars. The theoretical H-R diagram is shown in Fig. 9.

UCL has a well-defined MS turn-off composed of the *Hipparcos* members HIP 67464 (ν Cen; B2IV), HIP 68245 (ϕ Cen; B2IV), HIP 68282 (ν^1 Cen; B2IV-V), HIP 71860 (α Lup; B1.5III), HIP 75141 (δ Lup; B1.5IV), HIP 78384 (η Lup; B2.5IV), and HIP 82545 (μ^2 Sco; B2IV), as well as “classical” members (but *Hipparcos* non-members) HIP 82514 (μ_1 Sco; B1.5Vp) and 73273 (β Lup; B2III)⁶. The variable star HIP 67472 (μ Cen; B2Vnpe) was excluded. Using the Bertelli et al. (1994) tracks, the mean age of the 7 turn-off *Hipparcos* members is 17 ± 1 Myr. Including the two “classical” members has negligible effect on the mean age estimate. Our MS turn-off age estimate

⁵“Classical” members are early-type stars which were included in Sco-Cen membership lists before the *Hipparcos* studies of dZ99.

⁶Note that the two *Hipparcos* non-members were found to be probable members by Hoogerwerf (2000) if the long-baseline ACT (HIP 73273) and TRC (HIP 82514) proper motions were used instead of the *Hipparcos* values.

for UCL is slightly older than de Geus et al.’s (14-15 Myr), and is close to the mean pre-MS ages that we found in §7.1 (15-22 Myr).

LCC lacks a well-defined turn-off, however we have enough early-B stars in the middle of their MS phase with which to make an age estimate. We estimate the age for LCC from the following main sequence B stars: HIP 59747 (δ Cru; B2IV), HIP 60823 (σ Cen; B2V), HIP 61585 (α Mus; B2IV-V), HIP 63003 (μ^1 Cru; B2IV-V), and HIP 64004 (ξ^2 Cen; B1.5V). The mean age for these five stars is 16 ± 1 Myr; similar to what we found for UCL, and it agrees well with the younger end of our pre-MS age estimates (17-23 Myr). This age estimate is significantly older than previous estimates (10-12 Myr), and warrants more critical examination (§8.3).

The new results yielded by our age analysis of the OB subgroups are: (1) two-thirds of the low-mass star-formation in each subgroup took place in less than a ~ 5 Myr span (and 95% took place within ~ 10 Myr), (2) the pre-MS and B-star ages for LCC and UCL are in approximate agreement, (3) the B-star subgroup memberships defined by *Hipparcos* have ages of 16 ± 1 Myr and 17 ± 1 Myr for LCC and UCL, respectively. We discuss the implications of these results in §8.

7.3. The Census of Accretion Disks

An important question both for star and planet formation is the lifetime of accretion disks around young stars. Statistics for the frequency of active accretion disks around low-mass stars come predominantly from near-IR surveys of young associations and clusters (Hillenbrand & Meyer 1999; Haisch, Lada, & Lada 2001). The samples of low-mass stars surveyed are dominated by embedded associations with ages of < 3 Myr (e.g. Tau-Aur, Cha I, etc.), and older open clusters with ages of 30-100 Myr (e.g. Pleiades, IC 2602, α Per, etc.). Few well-studied pre-MS stars of 3-30 Myr-old ages have been surveyed. The situation has recently been slightly ameliorated by the discoveries of the TW Hya association and η Cha cluster (Kastner et al. 1997; Webb et al. 1999; Mamajek et al. 1999). Yet these samples are small (~ 10 -20 stars) and dominated by K and M-type stars with masses of 0.1 - $0.8 M_\odot$. Our pre-MS star sample is unique in its mass (~ 1 - $1.5 M_\odot$) and age range (~ 10 -20 Myr), so measuring its disk-

frequency provides a valuable datum.

Stars with $\text{EW}(\text{H}\alpha) > 10\text{\AA}$ in emission are usually called Classical T Tauri stars (CTTSs), which show spectroscopic signatures of accretion as well as near-IR excesses (e.g. Hartigan, Edwards, & Ghandour 1995). Stars lacking the strong $\text{H}\alpha$ emission and near-IR excesses are called Weak-lined T Tauri stars (WTTSs). This can be explained as a correlation between the presence of magnetospheric accretion columns and an inner accretion disk (e.g. Meyer, Calvet, & Hillenbrand 1997; Muzerolle, Hartmann, & Calvet 1998). Our $\text{H}\alpha$ EW measurements are discussed in §4.2.1, and here we quantify the K-band excess of our targets. We calculate the intrinsic $J - K$ color excess $E(J - K)_\circ$ as defined by Meyer, Calvet, & Hillenbrand (1997):

$$E(J - K)_\circ = (J - K)_{\text{obs}} - (J - K)_\circ - A_V \times (A_J - A_K) \quad (1)$$

where $(J - K)_{\text{obs}}$ is the observed color and $J - K_\circ$ is the intrinsic color of an unreddened dwarf star of appropriate spectral type (Kenyon & Hartmann 1995). Uncertainties in each quantity were propagated in order to estimate the signal-to-noise of the intrinsic color excess. The distribution of measured $E(J - K)_\circ$ values indicate a systematic offset of a few hundredths of a mag. Our near-IR data set is from the 2MASS working database, so we suspect that the absolute calibration or uncertainties in color correction could be responsible and apply a small color correction to account for it. After the correction, the distribution of $E(J - K)_\circ$ values is symmetric about zero, with a few positive and negative $\sim 2\sigma$ points. There is only one star with a $E(J - K)_\circ$ color excess with $\text{S/N} > 2.5$: star #34 = TYC 9246-971-1 has an intrinsic color excess of $E(J - K)_\circ = 0.26 \pm 0.06$ implying a K-band excess. This star also happens to be the only CTT identified in our optical spectra ($\text{EW}(\text{H}\alpha) = -39\text{\AA}$). TYC 9246-971-1 (= PDS 66, Hen 3-892) was originally identified as an emission line star by Henize (1976), and classified as a CTT in the Pico dos Dias survey of stars in the IRAS PSC catalog (Gregorio-Hetem et al. 1992). By virtue of its position, proper motion, and spectral characteristics, we find that TYC 9246-971-1 is a ≈ 8 Myr-old, $\approx 1.2 M_\odot$ (DM97 tracks) member of the LCC subgroup. Our secular parallax for TYC 9246-971-1

yields a distance of 86^{+8}_{-7} pc ; the third nearest of the LCC pre-MS stars in our sample, and among the nearest CTTSs known. Only 1/58 ($1.7^{+4.0}_{-1.4}\%$; 1σ Poisson) of pre-MS stars in LCC are classified as bona fide CTTS, along with none (0/42) of the pre-MS members of UCL. For our accretion disk frequency statistics, we use the isochronal ages derived from the DM97 evolutionary tracks (which agree well with the turn-off ages), and include the entire sample of 110 pre-MS stars (including the cooler stars which bias the mean to younger ages). Only 1/110 ($0.9^{+2.1}_{-0.8}\%$; 1σ) of $1.3 \pm 0.2 (1\sigma) M_\odot$ stars with ages of 13 ± 1 (s.e.) ± 6 (1 σ) Myr are CTTSs. This implies that accretion terminates in solar-type stars within the first 15 Myr of their evolution.

8. Discussion

We can address several interesting questions regarding the star-formation history of Sco-Cen with data from our survey. Could the Sco-Cen progenitor giant molecular cloud (GMC) have produced a substantial population of low-mass stars for an extended period ($> 5\text{-}10$ Myr) *before* conditions were right to form an OB population? Conversely, is there evidence for any low-mass star-formation *after* the bulk of the high-mass OB stars formed? The OB star-formation in LCC and UCL has apparently destroyed the progenitor GMC through supernovae and stellar winds (e.g. de Geus 1992; Preibisch & Zinnecker 2000). However the region is not totally devoid of molecular gas (e.g. the Lupus complex). We will first examine whether there is any evidence of star-formation prior to the formation of the OB subgroups (§8.1), and then assess the evidence for more recent star-formation in the UCL region (§8.2). We will address the age of LCC in §8.3, and discuss the formation of the subgroups in §8.4. Throughout the discussion, we adopt the DM97 ages, as they agree more closely with the turn-off ages than do the SDF00 and PS01 ages.

8.1. Is There Evidence for Star-Formation Before the Primary Bursts?

Is our survey sensitive to older stars which may have preceded the primary star-formation episode? Three pre-MS stars in our sample have isochronal ages of > 25 Myr (or undefined as lying

below the ZAMS), however given the uncertainties in T_{eff} and $\log L/L_\odot$ (Fig. 5), even a co-eval ≈ 15 Myr-old population would be expected to have *statistical* outliers. Here we explore three possible ways in which older ZAMS stars could have escaped our attention.

One could argue that our surface gravity indicator is biasing our sample against identifying ZAMS stars members (if they exist). If we disregard surface gravity as a criterion, we gain only 4 more RASS-ACT/TRC stars (all between F8.5 and G1), and only *one* of those would have an isochronal age > 25 Myr (TYC 8222-105-1; ~ 30 Myr). If they were legitimate, older members with real ages of > 25 Myr, they should also be among the stars with the oldest *isochronal ages* in our sample, which they are not. This suggests that their secular parallaxes, hence their luminosities, are unjustified, and that they are not members of the OB subgroups. Coincidentally, TYC 8222-105-1 is one of the earliest type stars in our sample (F8.5), where our surface gravity indicator has the least fidelity (Fig. 1). We can state that only *one* of the Li-rich stars showing dwarf gravity signatures that is co-moving with LCC and UCL has an H-R diagram position and gravity suggestive of ZAMS status.

If a significant ZAMS population existed in LCC and UCL, would our magnitude and X-ray flux limits allowed their detection? X-ray surveys of the ZAMS-age clusters IC 2602 and IC 2391 (~ 30 -50 Myr) by Randich et al. (1995) and Patten & Simon (1996) found that late-F and early-G stars ZAMS stars have X-ray luminosities of $L_X \simeq 10^{29.0} - 10^{30.5}$ erg s $^{-1}$, with L_X/L_{bol} ranging from $10^{-3.0}$ to $10^{-4.8}$. The X-ray and optical flux limits imposed by the *ROSAT* All-Sky Survey and the Tycho catalog allow us to detect ZAMS sources with $L_X/L_{bol} > 10^{-3.2}$ within 140 pc if they exist. If we adopt the X-ray luminosities of the G stars in IC 2602 and IC 2391 as representative for a ~ 30 Myr-old population, we should have detected roughly one-third of a putative Sco-Cen ZAMS population between masses of 1 and $1.2 M_\odot$. We can put a rough upper limit on the number of > 25 Myr-old stars in our mass range. Assuming that TYC 8222-105-1 is a ZAMS member, and that its H-R diagram position is not a statistical fluctuation from the locus of ~ 15 Myr-old stars, we detect one ZAMS star with age > 25

Myr in the mass range ($1-1.2 M_\odot$). Accounting for the two-thirds of the ZAMS stars which would have undetectable X-ray emission, and extrapolating over a Kroupa (2001) IMF, this implies a population of ~ 100 stars with masses greater than $0.1 M_\odot$. This is $\leq 10\%$ of the stellar population predicted to exist in each OB subgroup (~ 1000 -2000; §5.3).

Could such ZAMS stars have left the region we probed? If we postulate that the population was very centrally concentrated and gravitationally bound until the OB stars destroyed the giant molecular cloud (GMC) some ~ 10 Myr ago (de Geus 1992), then a 2 km s^{-1} motion radially away from the subgroup center would have moved the star 20 pc in the past 10 Myr. This distance is the approximate radius of both of the subgroups today (see Fig. 9 of dZ99). Hence if an older population was concentrated at center of the gravitationally-bound GMC until the high mass stars destroyed the cloud, we would find them within the projected boundaries of the subgroups so long as they inherited velocities of $< 2 \text{ km s}^{-1}$. The kinematic selection procedure of Hoogerwerf (2000) would have selected such stars, since a large velocity dispersion (3 km s^{-1}) was initially assumed.

We conclude that there is no evidence for significant star-formation in the LCC and UCL progenitor giant molecular clouds before the primary star-formation episodes. Our findings are consistent with the idea that molecular clouds form stars over a range of masses, and dissipate within timescales of ~ 10 Myr.

8.2. On-going Star-Formation?

Two obvious sources of young stars may be contaminating the UCL pre-MS sample. The youngest, unembedded OB subgroup of Sco-Cen is US, with a nuclear age of 5-6 Myr (de Geus et al. 1989). US borders UCL near Galactic longitude 343° , and its space motion and distance are very similar to that of UCL (dZ99). The Lupus molecular clouds are also in the western region of UCL (roughly between $335^\circ < \ell < 345^\circ$ and $+5^\circ < b < 25^\circ$). The T Tauri star population within the major Lupus clouds was surveyed by Hughes et al. (1994), and the region was recently mapped in ^{12}CO by Tachihara et al. (2002). Dozens of pre-main sequence stars were identified outside of the main cores by a pointed *ROSAT* survey (Kraut-

ter et al. 1997), and the All-Sky Survey (Wichmann et al. 1997b). The clouds lie at $d = 140$ pc (Hughes, Hartigan, & Clampitt 1993), situated spatially between the US and UCL subgroups of Sco-Cen (both $d \simeq 145$ pc). Fig. 10 illustrates the positions of the primary Lupus clouds, the pre-*ROSAT* Lupus T Tauri star population, the pre-MS stars from our survey, and the B-star population of the OB subgroups.

How does the presence of US and the Lupus molecular clouds (and their associated T Tauri stars) affect our findings regarding the mean age of the UCL subgroup? We split our unbiased ($\log T_{eff} > 3.73$) “pre-MS” and “pre-MS?” members of UCL into two groups using the Galactic longitude line 335° as a division. Most of the molecular cloud mass in the Lupus region lies between $335^\circ < \ell < 345^\circ$ (see Fig. 2 of Tachihara et al. (2002)). Using the DM97 tracks, we find that the “eastern” UCL pre-MS sample surrounding the Lupus clouds has a mean age of 13 ± 1 Myr, while the “western” UCL sample is somewhat older (16 ± 1 Myr). The UCL stars with ages of < 10 Myr are found in greater numbers near the Lupus clouds and US border, supporting the idea that our UCL sample is probably contaminated by more recent star-formation. The age estimate of UCL for the stars west of $\ell = 335^\circ$ is probably more representative of the underlying UCL population.

Three of the youngest stars (HIP 81380, TYC 7858-830-1, and TYC 7871-1282-1; 5-9 Myr; DM97 tracks) in our entire survey are positioned near a clump of 8 B stars at $(\ell, b) = (343^\circ, +4^\circ)$. These three pre-MS stars also have secular parallax distances of ~ 200 pc, similar to what de Bruijne (1999b) found for the group of B stars. The secular parallaxes may be biased, however, if this clump has slightly different kinematics than the average UCL motion. This clump may represent substructure within UCL. However de Bruijne (1999b) was unable to demonstrate that the clump had distinct kinematics or age. The mean *Hipparcos* distance of the clump B stars is 175 pc, with HIP 82514 (μ^1 Sco; B1.5Vp) and HIP 82545 (μ^2 Sco; B2IV) as the most massive members. Our identification of 3 new pre-MS stars in the same region with similar secular parallaxes supports the notion that this may be a separate subgroup.

Some of our pre-MS stars were also identified in

the *ROSAT* surveys of the Lupus region by Krautter et al. (1997) and Wichmann et al. (1997b) (see notes in Table 6). The presence of a significant population of pre-MS stars outside of star-forming molecular clouds has been attributed by various authors to be due to one or more of the following: (1) slow diffusion ($1-2 \text{ km s}^{-1}$) from existing molecular clouds (e.g. Wichmann et al. 1997a), (2) ejection from small-N body interactions (Sterzik & Durisen 1995), (3) formation *in situ* from short-lived clouddlets (Feigelson 1996), or (4) fossil star-formation associated with the Gould Belt (e.g. Guillout et al. 1998). Wichmann convincingly showed that most of the young RASS stars in the Lupus region are at a distance of around ~ 150 pc (similar to previously published distances for the Lupus clouds and UCL), and that the stars are roughly 10 Myr-old. Wichmann concludes that the dispersed pre-MS population is most likely a manifestation of the Gould Belt. The OB subgroups of Sco-Cen are major sub-structures of the Gould Belt (as defined by age and kinematics; Frogel & Stothers 1977), i.e. UCL is the dominant Gould Belt substructure in the Lupus region. We interpret the presence of dozens of pre-MS stars near the Lupus clouds to be primarily the low-mass membership of the UCL OB subgroup. Our analysis suggests that younger US or Lupus stars are a minor contaminant to our UCL sample.

8.3. Is LCC Older than UCL?

Although our pre-MS and turn-off age estimates for LCC agree rather well, they are substantially older (by $\sim 50\%$) than previous values. The de Geus et al. (1989) age estimate (11-12 Myr) appears to hinge primarily on the H-R diagram position of ϵ Cen, with δ Cru, α Mus, and ξ^2 Cen defining the rest of the turn-off isochrone. The latter three stars were confirmed as members by dZ99, however ϵ Cen (the most massive) was rejected. Although our age for ϵ Cen is consistent with de Geus’s, we omitted it from our LCC age estimate. If one uses the long-baseline proper motion for ϵ Cen from the new Proper Motions of Fundamental Stars (PMFS) catalog (Gontcharov et al. 2001), and adopt the LCC space motion, convergent point, and formulae of dZ99 (with $v_{int} = 3 \text{ km s}^{-1}$), ϵ Cen has a 100% membership probability. The resulting secular parallax ($\pi_{sec} = 9.6 \pm 2.0$ mas) agrees well with the *Hippar-*

\cos astrometric parallax ($\pi_{HIP} = 8.7 \pm 0.8$ mas), further strengthening the interpretation that ϵ Cen is a bona fide LCC member. Including ϵ Cen with the other 5 turn-off stars discussed in §7.2 does not change our turn-off age estimate, however (16 ± 1 Myr). If one ignores the stars with masses less than that of ϵ Cen, then the 12-Myr Bertelli isochrone would appear to be an acceptable fit for LCC. Because the turn-off is poorly defined, we give equal weight to the next five *Hipparcos* members down the mass spectrum (δ Cru, σ Cen, α Mus, μ^1 Cru, and ξ^2 Cen), which yields an age older than de Geus's.

ϵ Cen is one of several “classical” LCC early B-type member candidates rejected as members of Sco-Cen using the *Hipparcos* astrometry. These stars have been included in Sco-Cen candidate membership lists on and off over the past half-century: HIP 59196 (δ Cen; B2IVne), HIP 60718A (α^1 Cru A; B0.5IV), HIP 62434 (β Cru; B0.5IV), and HIP 68702 (β Cen; B1III). These stars are $\sim 10\text{-}20 M_\odot$ star, with inferred ages of $\sim 5\text{-}15$ Myr, and distances of $\sim 100\text{-}150$ pc. Such stars are extremely rare, and their presence in the LCC region appears to be more than coincidental. Are they all LCC members whose *Hipparcos* proper motions are perturbed due to binarity? All five systems are flagged (field #59) in the *Hipparcos* catalog as stars with unusual motions due to either unseen companions or variability. A kinematic investigation of these stars, and their potential membership in LCC is beyond the scope of this study, but necessary for understanding the global star-formation history of the Sco-Cen region. Are these stars bona fide members? If so, why are they so much younger than the other members (both pre-MS and mid-B stars)? If they are not bona fide members, where did they come from? Although our age estimates for the pre-MS sample and *Hipparcos* early-B members appear to be consistent, the presence of these young, B0-B2 classical members (*Hipparcos* non-members) hints that the story of star-formation in Sco-Cen is more complex than our results reveal.

8.4. A Star-Formation History of Sco-Cen?

Preibisch & Zinnecker (2000) reviewed the recent star-formation history of Sco-Cen ($<5\text{-}10$ Myr) in the region of US, UCL, and ρ Oph. They

present evidence for external supernovae triggering in the formation of the subgroups. They claim that supernovae shock waves from UCL passed through the US progenitor GMC approximately 5 Myr ago, and caused the cloud to collapse. The US group appears to have had at least one supernova in the past ~ 1 Myr, possibly a deceased massive companion to the runaway O9.5V star ζ Oph. This supernova contributed to destroying the GMC and producing the US superbubble (de Geus 1992; Hoogerwerf, de Brujne, & de Zeeuw 2001). The US subgroup appears to be currently triggering star-formation in the ρ Oph cloud core. Here we speculate on the global star-formation history of the Sco-Cen complex.

The formation of LCC and/or UCL may have been similarly triggered. However it is unclear if one triggered the formation of the other or vice versa. Our pre-MS age estimates are consistent with LCC being slightly older than UCL by a few Myr, though they could be coeval. What was the origin of these large OB subgroups? The gas associated with the Sco-Cen complex appears to be part of the Lindblad Ring, a torus of H I and molecular clouds hundreds of pc in radius. It is centered roughly near the α Persei cluster and Cas-Tau OB association (Blaauw 1991; Pöppel 1997). The young stars that have formed from this gas complex (i.e. the Gould Belt) share a systematic expansion consistent with a localized origin for the whole complex – probably an expanding gas shell from a large star-formation event (e.g. Moreno, Alfaro, & Franco 1999). The gas associated with Sco-Cen appears to be part of a “spur” of neutral hydrogen and molecular clouds that runs from near LCC (including Coalsack, Musca, and Chamaeleon clouds), through Lupus, Ophiuchus, and into the Aquila and Vulpecula Rift regions (see Fig. 3-18 of Pöppel 1997). It is likely that LCC and UCL were among the first clumps in the Lindblad Ring to collapse and form stars (see §4 of Blaauw 1991), either from self-gravity or from triggered from external supernovae events. The LCC and UCL regions formed a large population of OB stars and their stellar winds and supernovae may indeed have triggered the collapse of the US group. The process might continue over the next 10 Myr as the supernovae from the US and ρ Oph subgroups send shock waves into the vast reservoir of atomic and molecular gas asso-

ciated with the Aquila Rift (see §3.4 of Pöppel 1997, and references therein). On the other side of Sco-Cen, there appears to be little gas westward of LCC until one reaches the Vela complex some 400 pc away. The lack of a sufficient gas reservoir probably explains why triggering did not proceed to form OB subgroups west of LCC.

The Sco-Cen subgroups have formed their own network of superbubbles with radii of ~ 100 pc (de Geus 1992). The superbubbles appear to be largely H I, presumably gas from the progenitor Sco-Cen GMC as well as the swept-up interstellar medium. In some regions, they are associated with well-known nearby molecular cloud complexes: Coalsack, Musca, Chamaeleon, Corona Australis, Lupus, and numerous small high Galactic latitude clouds (e.g. Bhatt 2000). The Lupus clouds are spatially coincident with the western side of the US superbubble, however no kinematic analysis has been yet undertaken to determine whether the Lupus clouds share in the bubble expansion. The CrA molecular clouds are embedded within the UCL superbubble shell, and the space motion of the T Tauri star population is moving radially away from UCL (Mamajek & Feigelson 2001). Other young stars in the field toward the 4th Galactic quadrant, including the η Cha cluster, TW Hya association, and β Pic group, all have ages of ~ 10 Myr and are moving radially away from LCC and UCL. Perhaps these stars formed in small molecular clouds that accumulated within the expanding LCC/UCL superbubble shells.

9. CONCLUSIONS

From our spectroscopic survey of an X-ray- and kinematically-selected sample of late-type stars in the Sco-Cen OB association, we summarize our main findings as follows:

- We have identified a population of low-mass stars in the Lower Centaurus-Crux (LCC) and Upper Centaurus-Lupus (UCL) OB subgroups with the following properties: (1) G-K spectral types, (2) subgiant surface gravities, (3) Lithium-rich, (4) strong X-ray emission ($L_X \simeq 10^{30} - 10^{31}$ erg s $^{-1}$), and (5) proper motions consistent with the high-mass members. We classify stars which show these characteristics as bona fide pre-MS stars or “post-T Tauri” stars. X-ray and

kinematic selection (the RASS-ACT/TRC sample) yielded a hit rate of 93% for selecting probable pre-MS stars, while kinematic selection alone (dZ99 *Hipparcos* sample G-K dwarfs and subgiants) yielded 73%.

- We estimate the mean age of the pre-MS population in the LCC subgroup to be 17 ± 1 Myr (DM97 tracks), 21 ± 2 Myr (PS01), and 23 ± 2 Myr (SDF00). For UCL, the pre-MS population’s mean age is 15 ± 1 Myr (DM97), 19 ± 1 Myr (PS01), and 22 ± 1 Myr (SDF00). The UCL pre-MS estimate appears to be slightly biased towards younger ages (by ~ 1 Myr) through contamination by Lupus or US members. We also calculate new MS turn-off ages of 16 ± 1 Myr for LCC and 17 ± 1 Myr for UCL using the dZ99 *Hipparcos* membership and Bertelli et al. (1994) evolutionary tracks. The UCL pre-MS and turn-off age estimates are roughly self-consistent, and similar to previously published estimates. Our age estimates for LCC (pre-MS and turn-off) are older than previous estimates, and are equal to or slightly older than UCL.
- We find that 68% of the low-mass star-formation in each subgroup took place within a $<4\text{--}6$ Myr span, and 95% took place within $<8\text{--}12$ Myr (using DM97 tracks). The conditions were right for producing low-mass stars in the LCC and UCL progenitor molecular clouds for <10 Myr.
- We find the frequency of CTTSs among a pre-MS population in an OB association with masses of 1.3 ± 0.2 (1σ) M_\odot and ages of 13 ± 1 (s.e.) ± 6 (1σ) Myr (DM97 tracks) to be only $0.9_{-0.8}^{+2.1}\%$ (1/110). The younger age results from using our entire (i.e. magnitude-biased) sample of pre-MS stars. Only one star in our sample showed both strong H α -emission and a K-band excess: the previously known CTTS TYC 9246-971-1 (#34 = PDS 66 = Hen 3-892). This suggests that the disk accretion phase lasts $\leq 10\text{--}20$ Myr in the evolution of solar-type stars in OB associations.
- We demonstrate that a surface gravity indicator for classifying field G and K stars

(Sr II λ 4077 to Fe I λ 4071) can be used to distinguish whether Li-rich stars are pre-MS or ZAMS in nature. When this indicator is used in tandem with other youth diagnostics (Li abundance, X-ray emission, H α emission, and kinematics), one can confidently classify a star as pre-MS in nature.

EM and MM acknowledge support through NASA contract 1224768 administered by JPL. EM and JL were also supported through a NASA/JPL grant. EM also thanks the $\Sigma\Xi$ Research Honor Society for a Grant-in-Aid which financed part of our observing run. We thank the TAC of the Mt. Stromlo and Siding Springs Observatories 2.3-metre telescope for their generous allocation of telescope time. This project benefited from discussions and help from J. Beiting, A. Blaauw, J. Carpenter, C. Corbally, J. de Bruijne, T. de Zeeuw, M. Hamuy, L. Hillenbrand, W. Lawson, D. Soderblom, J. Stauffer, and S. Strom. We offer special thanks to Ronnie Hoogerwerf for assistance in the target selection effort and discussions. This publication makes use of data products from the Two Micron All Sky Survey (2MASS), which is a joint project of the Univ. of Massachusetts and the Infrared Processing and Analysis Center (IPAC), funded by NASA and NSF.

A. The Pre-Main Sequence T_{eff} Scale

Pre-main sequence stars lie between dwarfs (V) and subgiants (IV) on color-absolute magnitude or temperature-luminosity H-R diagrams. A given visual spectral type will correspond to cooler temperatures as surface gravity decreases (e.g. Gray 1991; de Jager & Nieuwenhuijzen 1987). Dwarf temperature scales are often adopted for pre-MS populations, however it is prudent to account for the effects of surface gravity.

We quantify the effects of $\log g$ on the SpT vs. T_{eff} relation using two datasets. First, we fit a polynomial surface to $T_{eff}(\text{SpT}, \log g)$ using the data from Gray (1991, Table 2). As with most compilations of $T_{eff}(\text{SpT})$ in the FGK-star regime, we find that a trinomial is the best low-order fit, and that a linear dependence on $\log g$ adequately accounts for the effects of surface gravity on temperature. Our second method finds a similar surface fit to $T_{eff}(\text{SpT}, \log g)$ using published T_{eff} and $\log g$ values (Cayrel de Strobel et al. 2001) for the GK standards of Keenan & McNeil (1989) and F standards of Garcia (1989) (those within 0.3 dex of solar [Fe/H], and luminosity class IV and V only). We adopt the isochrones from D'Antona & Mazzitelli (1997) for a fiducial $\log g$ value as a function of T_{eff} for a coeval 15-Myr-old population.

Both assessments yield essentially the same result: dwarf temperature scales for G-K stars should be lowered by 35 K for a 15 Myr-old population. The temperature decrement increases for younger ages: 70 K-40 K for G0-K2 10-Myr-old stars, 235 K-105 K for G0-K2 5-Myr-old stars, and 260 K-180 K for G3-K2 1-Myr-old stars. Both techniques yielded a linear dependence of $\log g$ on $T_{eff}(\text{SpT}, \log g)$, and the slopes were similar: $\partial T_{eff}/\partial \log g \simeq 220 \text{ K}/\log(\text{cm s}^{-1})$ for the Keenan standards with Cayrel de Strobel stellar atmosphere data, and $\partial T_{eff}/\partial \log g \simeq 190 \text{ K}/\log(\text{cm s}^{-1})$ for the interpolation of Gray's (1991) Table 2. As the evolutionary model isochrones are parallel to the main sequence when the stars are on the radiative tracks (i.e. \sim 10-30 Myr for $\sim 1 M_{\odot}$ stars), the $\Delta \log g$ between a 15 Myr-isochrone and the main sequence is fairly constant over the G-K spectral types. Hence one naively expects a linear offset in $T_{eff}(\text{SpT}, \log g)$ between the 15-Myr isochrone and the MS.

With the 1σ scatter between published $T_{eff}(\text{SpT})$ relations being \sim 60 K amongst G stars, the systematic shift is nearly negligible. Upon comparing several temperature scales from the literature, we adopt the dwarf T_{eff} scale from Schmidt-Kaler (1982), and apply a -35 K offset to correct for the effects of lower surface gravity for a putative 15-Myr-old population. We conclude that adopting dwarf T_{eff} vs. SpT scales for pre-MS stars younger than \sim 10 Myr will systematically overestimate their T_{eff} values, and in turn, their masses inferred from evolutionary tracks. This could have deleterious systematic effects on derived initial mass functions for young associations.

B. Standards with Questionable Luminosity Class

Several of the standard stars we observed had H-R diagram positions, published $\log g$ values, and Sr II $\lambda 4077/\text{Fe I } \lambda 4071$ ratios (SrFe) which differed from what is expected for their luminosity classes given in Keenan & McNeil (1989). The differences are only at the half of a luminosity-class level. We adopt the Keenan temperature types for all of his standard stars, however we revised the luminosity classes of these stars to bring their H-R diagram positions, SrFe index, and published $\log g$ estimates into harmony (Table 9). The SrFe indices for the vast majority of the standards formed loci according to luminosity class (Fig. 1), so we are comfortable using the index as an additional discriminant. The dwarf regression line in the gravity indicator vs. temperature indicator plot (Fig. 1) was constructed using only Keenan standards for which his luminosity classification agreed with published $\log g$ values and the H-R diagram position.

C. Polynomial Fits

- *MI6 vs. Spectral Type*: This flux ratio is Index 6 of Malyuto & Schmidt-Kaler (1997). We measure the index in magnitudes ($MI6 = -2.5\log(f(\lambda\lambda 5125-5245)/f(\lambda\lambda 5245-5290)))$), and find the following relation for Keenan and Garcia F0-K6 III-IV standards (Table 3) within 0.3 dex of solar metallicity:

$$SpT = 33.26 \pm 0.07 + (22.75 \pm 0.48) \times MI6 \quad (0.06 < MI6 < 0.26) \quad (C1)$$

$$SpT = 30.82 \pm 0.16 + (105.38 \pm 8.28) \times MI6 - (711.74 \pm 173.81) \times MI6^2 \quad (-0.04 < MI6 < 0.06) \quad (C2)$$

where SpT is the spectral type on Keenan's (1984) scale, i.e. F5 = 28, F8 = 29, G0 = 30, G2 = 31, G5 = 32, G8 = 33, K0 = 34, K1 = 35, and K2 = 36. Intermediate types can be assigned e.g. G9 = 33.5, G9.5 = 33.75, K0+ = 34.25, K0.5 = 34.5, etc. The first equation applies to K0-K6 stars, and the second equation applies to F0-K0 stars. The 1σ dispersion in these fits is 0.6 subtypes.

- $\lambda 4374/\lambda 4383$ vs. *Spectral Type*: This band ratio consists of two 3Å bands centered on 4374.5Å and 4383.6Å. We measure the index in magnitudes as $YFe = -2.5 \times \log(f(\lambda 4374.5)/f(\lambda 4383.6))$. We find the following relation between the band ratio and SpT for F0-K6 III-V stars:

$$SpT = 25.97 \pm 0.30 + (20.47 \pm 0.90) \times YFe \quad (C3)$$

The residual standard deviation to the fit (using 20 Keenan F0-K5 III-V standards within 0.3 dex of solar metallicity) is 0.6 subtypes.

- *Surface Gravity Index Fe I $\lambda 4071/Sr II \lambda 4077$ vs. Spectral Type*: We measure a surface gravity index using the flux ratio of two 3Å bands centered on Fe I $\lambda 4071.4$ and Sr II $\lambda 4076.9$. We measure the flux ratio in magnitudes: $SrFe = -2.5 \times \log(f(\lambda 4071)/f(\lambda 4077))$, and plot against our MI6 spectral type index. The Keenan standard dwarfs confirmed as being main sequence stars define a narrow locus:

$$SrFe = -0.078 \pm 0.005 + (2.123 \pm 0.261) \times MI6 - (8.393 \pm 2.945) \times MI6^2 + (15.487 \pm 8.672) \times MI6^3 \quad (C4)$$

The 1σ sample standard deviation of this fit is 0.0094 mag in SrFe. The boundary between dwarfs and subgiants in Fig. 1 is -2σ of the dwarf locus. This relation is valid for F9-K6 stars.

- *H α vs. Spectral Type*: In Fig. 2, we fit the equivalent widths of the H α feature (at low resolution, the photospheric absorption plus the chromospheric emission) as a function of spectral type for F0-K6 dwarf and subgiant standard stars (Table 3) with the following polynomial:

$$EW(H\alpha) = 2.983 \pm 0.066 - (0.456 \pm 0.027) \times (SpT - 30) + (2.574 \pm 0.378) \times 10^{-2} \times (SpT - 30)^2 \quad (C5)$$

$EW(H\alpha)$ is measured in Å. SpT is spectral type on Keenan's scale (as before). The sample standard deviation of the polynomial fit to 11 standards was 0.20Å.

- *Converting Tycho $B-V$ to Cousins-Johnson $B-V$* : The *Hipparcos* catalog gives linear relations between $B_T - V_T$, $B - V$, V , and V_T for stars of a wide range in spectral types. Bessell (2000) compared the *Hipparcos*/Tycho photometry and that of the E-region photometric standards, and refined the relations between the two systems. Table 2 of Bessell (2000) gives a standard relation between $B_T - V_T$, Cousins-Johnson $B - V$, and $(V - V_T)$ for B-G dwarfs and K-M giants. We fit the following relations to Bessell's tables:

$$V = V_T + 9.7 \times 10^{-4} - 1.334 \times 10^{-1}(B_T - V_T) + 5.486 \times 10^{-2}(B_T - V_T)^2 - 1.998 \times 10^{-2}(B_T - V_T)^3 \quad (C6)$$

$$B - V = (B_T - V_T) + 7.813 \times 10^{-3}(B_T - V_T) - 1.489 \times 10^{-1}(B_T - V_T)^2 + 3.384 \times 10^{-2}(B_T - V_T)^3 \quad (C7)$$

$$B-V = (B_T - V_T) - 0.006 - 1.069 \times 10^{-1}(B_T - V_T) + 1.459 \times 10^{-1}(B_T - V_T)^2 \quad (C8)$$

The $V(V_T, B_T - V_T)$ polynomial equation C6 applies to stars from $-0.25 < (B_T - V_T) < 2.0$ (B-M types). Equation C7 is for stars with $0.5 < (B_T - V_T) < 2.0$, and equation C8 is for stars with $-0.25 < (B_T - V_T) < 0.5$. We do not quote uncertainties in the polynomial coefficients since the Bessell relations are already smoothed. These equations fit Bessell's standard relations to 1-2 millimagnitudes.

REFERENCES

Balona, L. A., 1994, MNRAS, 268, 119

Basri, G., Marcy, G. W., & Graham, J. R., 1996, ApJ, 458, 600

Bertelli, G., Bressan, A., Chiosi, C., Fagotto, F., & Nasi, E., 1994, A&AS, 106, 275

Bertout, C., 1989, ARA&A, 27, 351

Bessell, M.S., 2000, PASP, 112, 961

Bessell, M.S. & Brett, J.M., 1988, PASP, 100, 1134

Bessell, M.S., Castelli, F., & Plez, B., 1998, A&A, 333, 231

Bhatt, H. C., 2000, A&A, 362, 715

Blaauw, A., 1946, Ph.D. Thesis, Groningen University

Blaauw, A., 1991, in The Physics of Star Formation and Early Stellar Evolution, NATO ASI Series C, Vol. 342, eds. C.J. Lada & N.D. Ky-lafis (Dordrecht: Kluwer), 125

Bouvier, J., Wichmann, R., Grankin, K., Allain, S., Covino, E., Fernandez, M., Martin, E. L., Terranegra, L., Catalano, S., Marilli, E., 1997, A&A, 318, 495

Carpenter, J.M., 2001, AJ, 121, 2851

Cayrel de Strobel, G., Soubiran, C., Ralite, N., 2001, A&A, 373, 159

Covino, E., Alcala, J. M., Allain, S., Bouvier, J., Terranegra, L., & Krautter, J., 1997, A&A, 328, 187

Crawford, D. L., 1978, AJ, 83, 48

Crawford, D. L. & Mandewala, N., 1976, PASP, 88, 917

Cutispoto, G., Pastori, L., Pasquini, L., de Medeiros, J. R., Tagliaferri, G., & Andersen, J., 2002, A&A, 384, 491

D'Antona, F. & Mazzitelli, I., 1997, Mem. Soc. Astr. Ital., 68, 807 (DM97)

de Bruijne, J. H. J., 1999a, MNRAS, 306, 381

de Bruijne, J. H. J., 1999b, MNRAS, 310, 585

de Geus, E., de Zeeuw, P. & Lub, J., 1989, A&A, 216, 44

de Geus, E., 1992, A&A, 262, 259

de Jager, C. & Nieuwenhuijzen, H., 1987, A&A, 177, 217

de Zeeuw, P. T. & Brand, J., 1985, in Birth and Evolution of Massive Stars and Stellar Groups; Proceedings of the Symposium, Dwingeloo, Netherlands, September 24-26, 1984, (Dordrecht: D. Reidel), 102

de Zeeuw, P. T., Hoogerwerf, R., de Bruijne, J. H. J., Brown, A. G. A., & Blaauw, A., 1999, AJ, 117, 354 (dZ99)

Drilling, J. S., & Landolt, A. U., 2000, in Allen's Astrophysical Quantities, 4th. Ed., ed. Arthur C. Cox, (New York: AIP Press, Springer)

European Space Agency, 1997, The Hipparcos and Tycho Catalogues, ESA SP-1200

Feigelson, E. D., 1996, ApJ, 468, 306

Fleming, T. A., Molendi, S., Maccacaro, T., & Wolter, A., 1995, ApJS, 99, 701

Frogel, J. A., & Stothers, R., 1977, AJ, 82, 890

Garcia, B., 1989, Bull. Inform. CDS 36, 27

Gehrels, N., 1986, ApJ, 303, 336

Gontcharov, G. A., Andronova, A. A., Titov, O. A., & Kornilov, E. V., 2001, A&A, 265, 222

Gray, D. F., 1991, The Observation and Analysis of Stellar Photospheres, 2nd ed., (New York: Cambridge)

Gray, R.O., 2000, A Digital Spectral Classification Atlas, <http://nedwww.ipac.caltech.edu/level5/Gray/>

Gray, R.O., Graham, P.W., & Hoyt, S.R., 2001, AJ, 121, 2159

Gregorio-Hetem, J., Lépine, J. R. D., Quast, G. R., Torres, C. A. O., & de la Reza, R., 1992, AJ, 103, 549

Guillout, P., Sterzik, M. F., Schmitt, J. H. M. M., Motch, C., & Neuhäuser, R., 1998, A&A, 337, 113

Haisch Jr., K. E., Lada, E. A., & Lada, C. J., 2001, *ApJ*, 553, L153

Hamuy, M., Suntzeff, N. B., Heathcote, S. R., Walker, A. R., Gigoux, P., & Phillips, M. M., 1994, *PASP*, 106, 566

Hartigan, P., Edwards, S., & Ghandour, L., 1995, *ApJ*, 452, 736

Hauck, B. & Mermilliod, M., 1997, *A&AS*, 129, 431

Henize, K. G., 1976, *ApJS*, 30, 491

Herbig, G. H., 1978, in *Problems of Physics and Evolution of the Universe*, ed. L. V. Mirzoyan (Yervan: Acad. Sci. Armenian SSR), 171

Herbig, G. H., Bell, K. Robin, 1988, *Lick Obs. Bulletin* No. 1111, (Santa Cruz: Lick Observatory)

Hillenbrand, L. A. & Meyer, M. R., 1999, *BAAS*, 195, #209

Høg, E., Fabricius, C., Makarov, V.V., Urban, S., Corbin, T., Wycoff G., Bastian U., Schwerkendiek P., Wicenec A. 2000a, *A&A*, 355, L27

Høg, E., Fabricius, C., Makarov, V.V., Bastian, U., Schwerkendiek, P., Wicenec, A., Urban, S., Corbin, T., Wycoff, G. 2000b, *A&A*, 357, 367

Høg, E., Kuzmin, A., Bastian, U., Fabricius, C., Kuimov, K., Lindegren, L., Makarov, V.V., & Roeser, S., 1998, *A&A*, 335, L65

Hoogerwerf, R. 2000, *MNRAS*, 313, 43

Hoogerwerf, R. & Aguilar, L. A., 1999, *MNRAS*, 306, 394

Hoogerwerf, R., de Bruijne, J. H., J., & de Zeeuw, P. T., 2001, 365, 49

Houk, N., 1978, *Michigan Catalogue of Two-Dimensional Spectral Types for HD Stars*. (Vol. 2, $-52^\circ < -40^\circ$), (Ann Arbor: Univ. Michigan)

Houk, N., 1982, *Michigan Catalogue of Two-Dimensional Spectral Types for HD Stars*. (Vol. 3, $-40^\circ < -26^\circ$), (Ann Arbor: Univ. Michigan)

Houk, N. & Cowley, A. P., 1975, *Michigan Catalogue of Two-Dimensional Spectral Types for HD Stars*. (Vol. 1, $-90^\circ < -53^\circ$), (Ann Arbor: Univ. Michigan)

Houk, N. & Smith-Moore, M., 1988, *Michigan Catalogue of Two-Dimensional Spectral Types for HD Stars*. (Vol. 4, $-26^\circ < -12^\circ$), (Ann Arbor: Univ. Michigan)

Houk, N. & Swift, C., 1999, *Michigan Catalog of Two-Dimensional Spectral Types for the HD Stars*. (Vol. 5, $-12^\circ < +5^\circ$), (Ann Arbor: Univ. Michigan)

Hughes, J., Hartigan, P., Clampitt, L., 1993, *AJ*, 105, 571

Hughes, J., Hartigan, P., Krautter, J., & Kelemen, J., 1994, *AJ*, 108, 1071

Jensen, E., 2001, in *Young Stars Near Earth: Progress & Prospects*, eds. R. Jayawardhana & T. Greene, *ASP Conf. Ser.* Vol. 244, (San Francisco: ASP), 3

Johnson, H. L. & Morgan, W. W., 1953, *ApJ*, 117, 313

Jones, B. F., Fischer, D., Shetrone, M., & Soderblom, D. R., 1997, *AJ*, 114, 352

Kastner, J. H., Zuckerman, B., Weintraub, D. A., & Forveille, T., 1997, *Science*, 227, 67

Keenan, P.C., 1984, in *The MK Process and Stellar Classification*, ed. R. F. Garrison, (Toronto: Univ. of Toronto), 29

Keenan, P.C. & Barnbaum, C., 1999, *ApJ*, 518, 859

Keenan, P.C. & McNeil, R.C., 1989, *ApJS*, 71, 245

Keenan, P.C. & McNeil, R.C. 1976, *An Atlas of Spectra of the Cooler Stars*, (Columbus: Ohio State Univ.)

Keenan, P.C. & Yorka, S.B., 1988, *Bull. Inform. CDS* 35, 37

Kenyon, S.J. & Hartmann, L., 1995, *ApJS*, 101, 117

Köhler, R., Kunkel, M., Leinert, C., & Zinnecker, H., 2000, *A&A*, 356, 541

Krautter, J., Wichmann, R., Schmitt, J.H.M.M., Alcalá, J.M., Neuhauser, R., & Terranegra, L., 1997, *A&AS*, 123, 329

Kroupa, P., 2001, *MNRAS*, 322, 231

Lowrance, P. J., Schneider, G., Kirkpatrick, J. D., Becklin, E. E., Weinberger, A. J., Zuckerman, B., Plait, P., Malmuth, E. M., Heap, S. R., Schultz, A., Smith, B. A., Terriere, R. J., & Hines, D. C., 2000, *ApJ*, 541, 390

Maeder, A., 1981, *A&A*, 101, 385

Malyuto, V. & Schmidt-Kaler, Th. 1997, *A&A*, 693, 699

Mamajek, E.E., Lawson, W.A. & Feigelson, E.D. 1999, *ApJ*, 516, L77

Mamajek, E.E., Feigelson, E.D., 2001, Young Stars Near Earth: Progress & Prospects, ASP Conf. Ser. Vol. 244, eds. R. Jayawardhana & T. Greene, (San Francisco: ASP), 104.

Mashonkina, L. & Gehren, T., 2001, *A&A*, 376, 232

Mathis, J. S., 1990, *ARA&A*, 28, 37

Meyer, M. R., Calvet, N., & Hillenbrand, L. A., 1997, *AJ*, 114, 288

Moreno, E., Alfaro, E. J., & Franco, J., 1999, *ApJ*, 522, 276

Muzerolle, J., Hartmann, L., & Calvet, N., 1998, *AJ*, 116, 455

Napiwotzki, R., Schönberner, D., & Wenske, V., 1993, *A&A*, 268, 653

Palla, F., & Stahler, S. W., 2001, *ApJ*, 553, 299 (PS01)

Pallavicini, R., Cerruti-Sola, M., & Duncan, D.K., 1987, *A&A*, 174, 116

Patten, B. H., & Simon, T., 1996, *ApJS*, 106, 489

Pojmanski, G., 1998, *Acta Astron.*, 48, 35

Pöppel, W., 1997, *Fund. Cosm. Phys.*, 18, 1

Popper, D. M., 1966, *AJ*, 71, 175

Preibisch, T. & Zinnecker, H., 1999, *AJ*, 117, 2381

Preibisch, T. & Zinnecker, H., 2000, in Stellar Clusters and Associations: Convection, Rotation, and Dynamos, ASP Conf., Vol.198., eds. by R. Pallavicini, G. Micela, and S. Sciortino, 219

Randich, S., Schmitt, J. H. M. M., Prosser, C. F., & Stauffer, J. R., 1995, *A&A*, 300, 134

Randich, S., Aharpour, N., Pallavicini, R., Prosser, C. F., & Stauffer, J. R., 1997, *A&A*, 323, 86

Randich, S., Gratton, R., Pallavicini, R., Pasquini, L., & Carretta, E., 1999, *A&A*, 348, 487

Rebull, L. M., Wolff, S. C., Strom, S. E., & Makedon, R. B., 2001, *ApJL*, in press

Rodgers, A. W., Conroy, P., & Bloxham, G., 1988, *PASP*, 100, 626

Rose, J.A., 1984, *AJ*, 89, 1238

Schmidt-Kaler, Th., 1982, in Landolt-Börnstein: Numerical Data and Functional Relationships in Science and Technology, eds. K. Schaifers & H. H. Voigt, (Berlin: Springer-Verlag)

Shobbrook, R. R., 1983, *MNRAS*, 205, 1215

Siess, L., Dufour, E. & Forestini, M., 2000, *A&A*, 358, 593 (SDF00)

Slawson, R. W., Hill, R. J., & Landstreet, J. D., 1992, *ApJS*, 82, 117

Smart, W. M., 1968, Stellar Kinematics, (London:Longmans)

Soderblom, D. R., Jones, B. F., Balachandran, S., Stauffer, J. R., Duncan, D. K., Fedele, S. B., & Hudon, J. D., 1993, *AJ*, 106, 1059

Soderblom, D. R., King, J. R., & Henry, T. J., 1998, *AJ*, 116, 396

Spangler, C., Sargent, A. I., Silverstone, M. D., Becklin, E. E., Zuckerman, B., 2001, *ApJ*, 555, 932

Stauffer, J. R., Caillault, J.-P., Gagné, M., Prosser, C. F., & Hartmann, L. W., 1994, *ApJS*, 91, 625

Sterzik, M. F., & Durisen, R. H., 1995, *A&A*, 304, L9

Tachihara, K., Toyoda, S., Onishi, T., Mizuno, A., Fukui, Y., & Neuhäuser, R., 2002, PASJ, in press.

Urban, S.E., Corbin, T.E., & Wycoff, G.L. 1998, AJ, 115, 2161

Voges, W., et al., 1999, A&A, 349, 389

Wallace, L., Hinkle, K., & Livingston, W. 1998, An Atlas of the Spectrum of the Solar Photosphere from 13,500 to 28,000 cm^{-1} (3570 to 7405 Å), (Tucson: NOAO)

Webb, R., A., Zuckerman, B., Platais, I., Patience, J., White, R. J., Schwartz, M. J., McCarthy, C., 1999, ApJ, 512, L63

Wichmann, R., Krautter, J., Covino, E., Alcalá, J. M., Neuhäuser, R., Schmitt, J. H. M. M., 1997, A&A, 320, 185

Wichmann, R., Sterzik, M., Krautter, J., Metanomski, A., & Voges, W., 1997b, A&A, 326, 211

Wilking, B. A., Lada, C. J., & Young, E. T., 1989, ApJ, 340, 823

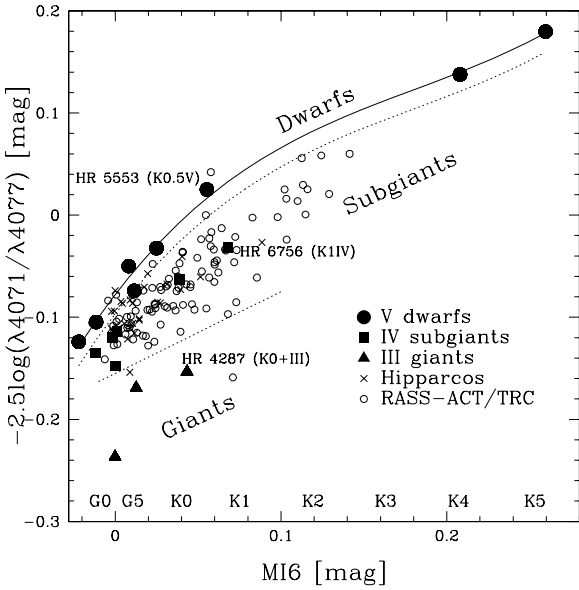


Fig. 1.— The MI6 band-ratio (T_{eff} indicator) vs. the band-ratio of Fe I $\lambda 4071$ / Sr II $\lambda 4077$ (surface gravity indicator). The solid line is a polynomial fit to only the dwarf standards. The dashed lines separate dwarfs, subgiants, and giants. The dwarf-subgiant dashed line is -2σ below the dwarf regression, whereas the subgiant-giant boundary is placed somewhat arbitrarily to resolve the observed subgiant and giant loci. Empirically, this diagram suggests that most of the target stars are consistent with being G and K-type subgiants, with few giant and dwarf interlopers. A few early-K standards are noted for reference.

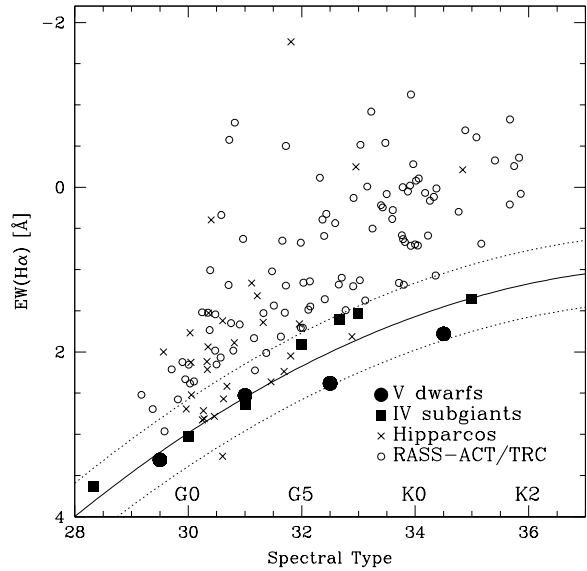


Fig. 2.— H α EWs for the pre-MS candidates compared to inactive field dwarfs and subgiants. Symbols are the same as for Fig. 1. The solid line is the average EW(H α) for dwarf and subgiant standard stars. The dashed line represents the $\pm 2\sigma$ residual scatter in the relation (encompassing all of the standards). Stars above this line are clearly chromospherically active, however those within the 2σ scatter have H α emission similar to older field stars.

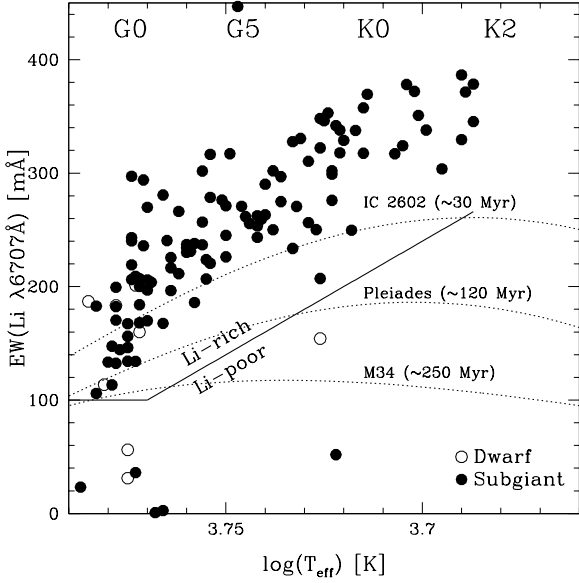


Fig. 3.— EWs for Li I $\lambda 6707$ for the program stars compared to regression fits for stars in young open clusters (see §4.2.2). We discuss assignment of dwarf and subgiant luminosity classes in §4.1.3. The pre-MS candidates form an obvious locus, and we select all stars above the solid line as “Li-rich”.

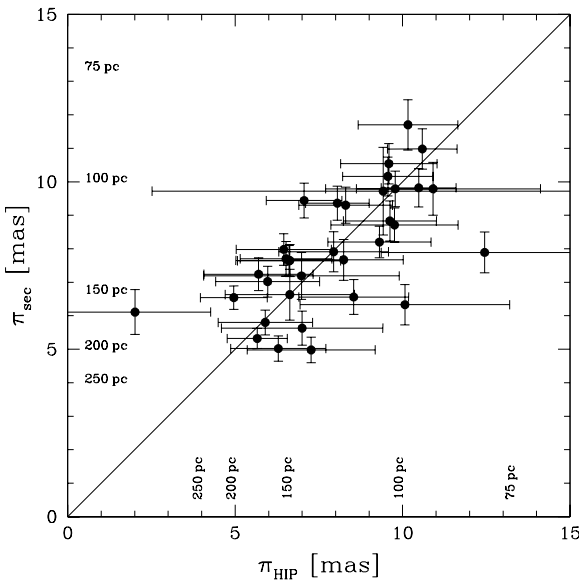


Fig. 4.— Comparison between *Hipparcos* astrometric parallaxes and our secular parallaxes calculated using the moving group method. Data points are Pre-MS (and Pre-MS?) association members from Tables 6 and 5.

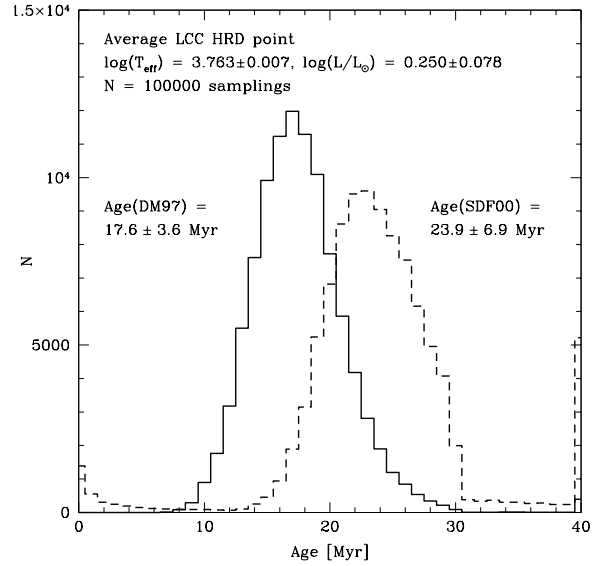


Fig. 5.— A histogram of the inferred ages from the DM97 and SDF00 tracks for a hypothetical LCC Pre-MS star with average H-R diagram point ($T_{eff}, \log L/L_{\odot}$) and gaussian uncertainties. The extreme right bin retains all points older than 40 Myr. The standard deviations are calculated using only stars with ages between 1-100 Myr.

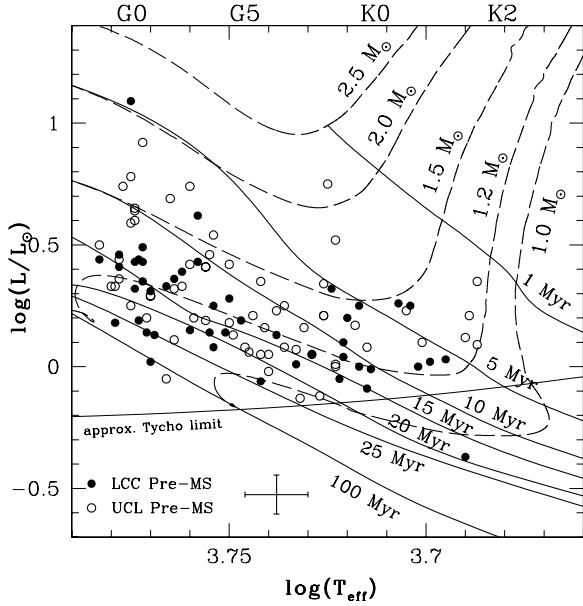


Fig. 6.— Theoretical H-R diagram for stars identified as Pre-MS or Pre-MS? in Tables 5 and 6 in the UCL (open circles) and LCC samples (filled circles). The pre-MS evolutionary tracks of DM97 are overlaid. The ACT/TRC magnitude limit ($V = 11$ mag) is shown for a distance of 150 pc ($A_V = 0.3$ assumed). The star in the bottom right corner (TYC 8648-446-1) is one of the faintest stars in our sample ($V = 11.2$ mag) with larger than average errors in $\log L/L_\odot$ - hence its unusual position. The average 1σ error bars in $\log T_{\text{eff}}$ and $\log L/L_\odot$ are shown.

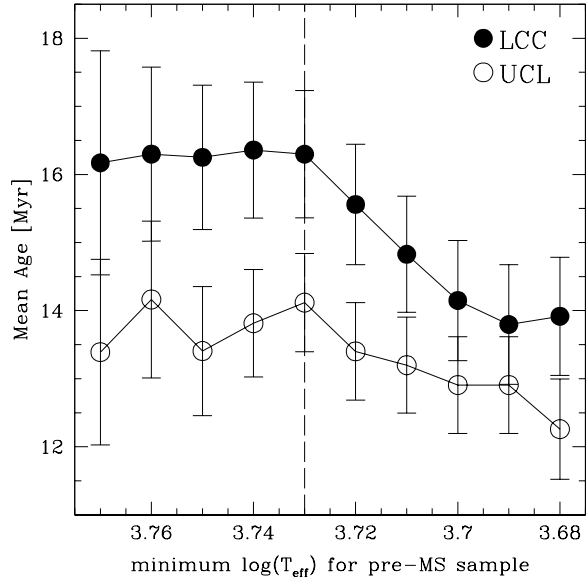


Fig. 7.— Illustration of the effects of magnitude bias on our mean age estimates for the pre-MS populations. The abscissa is the minimum $\log(T_{\text{eff}})$ threshold for evaluating the mean sample ages (using DM97 tracks). The ordinate is calculated mean age with standard errors of the mean (shown; typically ≈ 1 Myr). At cooler temperatures (later than K0), the magnitude limit of our survey biases the sample towards more luminous stars, thereby decreasing the mean age estimate. From this diagram, we choose $\log T_{\text{eff}} = 3.73$ (vertical dashed line) as the lower T_{eff} cut-off for evaluating the mean pre-MS ages. Known spectroscopic binaries are included here, but excluded in the final age estimates presented in Table 8. The *observed* isochronal ages and spread are 16 ± 5 Myr for LCC and 14 ± 5 Myr for UCL.

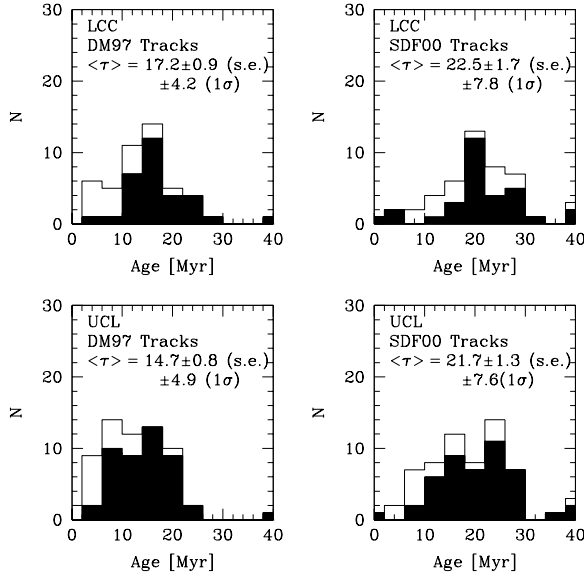


Fig. 8.— Histograms of the isochronal ages for pre-MS and “pre-MS?” candidates in Tables 5 and 6 from the models of DM97 and SDF00. The filled bins are for stars with $\log T_{eff} > 3.73$, and the unfilled bins are for the entire (magnitude-biased) sample. Mean isochronal ages (with standard errors of the means and 1σ uncertainties) are given for the unbiased sample ($\log T_{eff} > 3.73$). Outliers with isochronal ages of >40 Myr are counted within the 40 Myr bin.

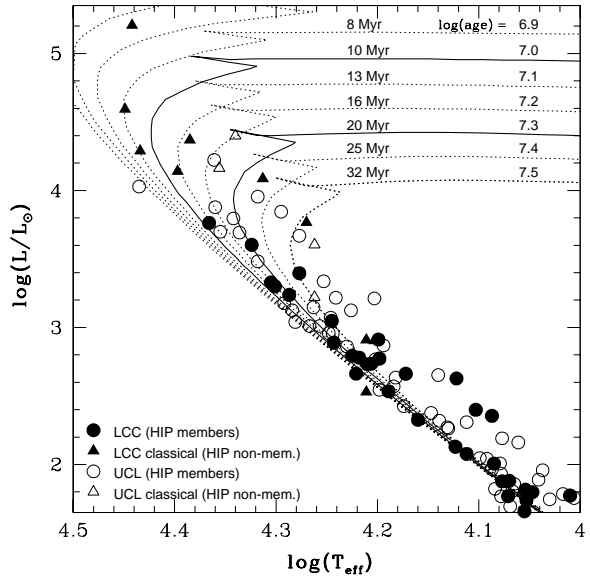


Fig. 9.— Theoretical H-R diagram for the B-star candidate members of the LCC & UCL memberships using the evolutionary tracks of Bertelli et al. (1994). Only the most massive *Hipparcos* members were included in the age estimates. The unusual variable HIP 67472 (μ Cen; B2Vnpe; $\log L/L_\odot$, $\log T_{eff} = 4.43, 4.0$) was excluded from the UCL turn-off age estimate.

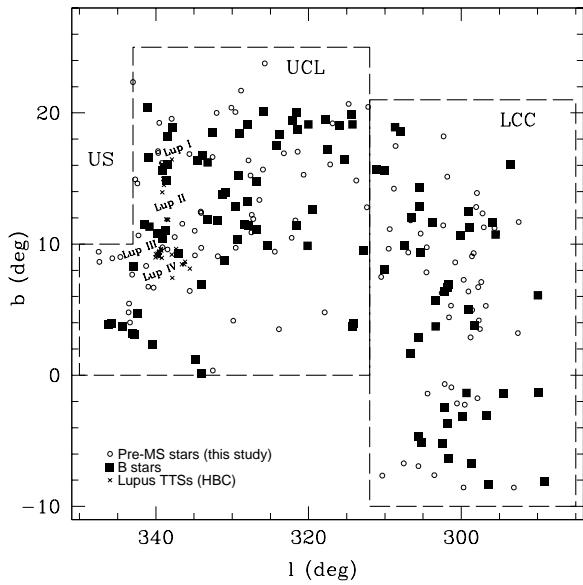


Fig. 10.— Map of the UCL and LCC subgroups of the Sco-Cen OB association (Sco OB2). The B-star population from de Zeeuw et al. (1999) is shown by filled squares. The pre-MS (and pre-MS?) sample from this survey is shown as open circles. Pre-*ROSAT* T Tauri stars in the HBC catalog associated with the Lupus cloud are shown as Xs (Herbig & Bell 1988).

TABLE 1
PROPERTIES OF DE ZEEUW *et al.* (1999) SCO-CEN G-K CANDIDATE MEMBERS

(1) Name HIP	(2) OB Grp.	(3) α h m s δ $^{\circ}, '$ $''$	(4) $\mu_{\alpha*}$, μ_{δ} (mas/yr)	(5) V	(6) $B - V$	(7) Spt MSS	(8) J (mag)	(9) H (mag)	(10) K _s (mag)	(11) notes
57524	LCC	11:47:24.55 -49:53:03.0	-33.7±0.8 -10.2±1.0	9.07	0.63±0.02	G3/5VPq2	7.91±0.02 7.59±0.06 7.51±0.02	1RXS J114724.3-495250, TWA 19A		
58996	LCC	12:05:47.48 -51:00:12.1	-37.5±0.8 -11.5±0.8	8.89	0.63±0.02	G1Vq1	7.67±0.01 7.37±0.03 7.27±0.01	var(0.06), 1RXS J120547.8-510007		
59854	LCC	12:16:27.84 -50:08:35.8	-29.1±1.3 -8.6±1.0	9.34	0.67±0.02	G3Vq1	8.04±0.01 7.35.8 -29.1±1.3 -8.6±1.0	9.34	0.67±0.02	7.69±0.02 7.61±0.03 1RXS J121627.9-500829
60885	LCC	12:28:40.05 -55:27:19.3	-34.9±0.8 -16.0±0.7	8.89	0.64±0.02	G1q4	7.68±0.02 7.40±0.05 7.28±0.03	var(0.02), 1RXS J122840.3-552707		
60913	LCC	12:29:02.25 -64:55:00.6	-37.5±1.2 -11.4±0.9	9.04	0.73±0.02	G5Vq1	7.60±0.01 7.26±0.01 7.14±0.01	...		
62445	LCC	12:47:51.87 -51:26:38.2	-30.4±1.0 -8.7±1.0	9.52	0.80±0.03	G8/K0Vq3	7.79±0.01 7.38±0.03 7.25±0.01	var(0.10), 1RXS J124751.7-512638		
63797	LCC	13:04:30.96 -65:55:18.5	-42.4±1.0 -14.2±0.8	8.48	0.74±0.01	G3Vq1	7.02±0.04 6.79±0.02 6.71±0.01	...		
63847	LCC	13:05:05.29 -64:13:55.3	-36.5±1.1 -19.5±1.3	9.18	0.73±0.02	G5Vq4	7.78±0.01 7.44±0.03 7.36±0.03	var(0.03)		
65423	LCC	13:24:35.12 -55:57:24.2	-29.0±1.0 -13.0±1.0	9.59	0.66±0.03	(G3w)F7q2	8.45±0.01 8.16±0.03 8.10±0.01	1RXS J132435.3-555719		
65517	LCC	13:25:47.83 -48:14:57.9	-39.0±1.2 -20.3±1.0	9.76	0.60±0.04	K0/2V+(G)q3	8.50±0.02 8.18±0.03 8.08±0.03	var(0.05, P=1.09d), V966 Cen, 1RXS J132548.2-481451		
66001	LCC	13:31:53.61 -51:13:33.1	-29.0±1.5 -20.1±1.1	9.84	0.72±0.04	G5/6Vq3	8.43±0.01 8.00±0.03 7.83±0.01	1RXS J133152.6-511335		
66941	LCC	13:43:08.69 -69:07:39.5	-32.7±0.7 -19.8±0.9	7.57	0.74±0.01	G2IV/Vq2	6.21±0.01 5.85±0.03 5.77±0.01	var(0.08), CCDM 1343-6908, 1RXS J134306.8-690754		
67522	UCL	13:50:06.28 -40:50:08.8	-29.3±1.5 -22.9±1.0	9.79	0.67±0.04	G1Vq2	8.58±0.01 8.30±0.04 8.16±0.02	1RXS J135005.7-405001		
68726	UCL	14:04:07.12 -37:15:50.5	-16.9±0.8 -16.7±0.7	7.11	0.72±0.02	G3IV/Vq3	5.29±0.00 5.40±0.04 4.92±0.05	CCDM 14041-3716		
71178	UCL	14:33:25.78 -34:32:37.7	-28.1±1.6 -28.0±1.4	10.18	0.81±0.06	G8/K0Vq3	8.52±0.01 8.06±0.02 7.94±0.02	var(0.15), V1009 Cen		
72070	UCL	14:44:30.96 -39:59:20.6	-20.9±1.5 -24.0±1.4	9.32	0.64±0.03	G3Vq3	8.19±0.01 7.93±0.02 7.81±0.01	...		
74501	UCL	15:13:29.22 -55:43:54.6	-16.1±0.8 -24.0±0.8	7.47	0.78±0.01	G2IVq1	5.86±0.01 5.48±0.02 5.20±0.01	...		
75924	UCL	15:30:26.29 -32:18:11.6	-31.7±2.4 -31.9±2.3	8.80	0.65±0.03	G6Vq2	7.37±0.01 7.05±0.03 6.92±0.02	1RXS J153026.1-321815		
76472	UCL	15:37:04.66 -40:09:22.1	-20.2±1.7 -27.6±1.4	9.39	0.73±0.03	G5Vq2	7.98±0.01 7.63±0.03 7.52±0.01	1RXS J153706.0-400929		
77015	UCL	15:43:29.86 -38:57:38.6	-20.5±1.6 -31.7±1.2	9.66	0.61±0.03	G3Vq1	8.61±0.01 8.34±0.03 8.32±0.02	...		
77081	UCL	15:44:21.05 -33:18:55.0	-19.1±1.8 -29.5±1.4	9.69	0.75±0.04	G8Vq2	8.27±0.02 7.86±0.03 7.79±0.02	...		
77135	UCL	15:44:57.69 -34:11:53.7	-20.6±3.3 -25.9±2.5	9.88	0.78±0.02	G6/G8IV/Vq3	8.43±0.02 8.04±0.02 8.23±0.04	CCDM 15450-3412, 1RXS J154458.0-341143		
77144	UCL	15:45:01.83 -40:50:31.0	-19.4±1.3 -31.1±1.4	9.46	0.57±0.03	G1Vq1	8.30±0.01 7.97±0.03 7.88±0.02	var(0.11), 1RXS J154502.0-405043		
77524	UCL	15:49:44.98 -39:25:09.1	-24.5±2.0 -25.2±1.8	10.64	1.09±0.12	K0(V)q3	8.81±0.01 8.27±0.02 8.13±0.02	1RXS J154944.7-392509		
77656	UCL	15:51:13.73 -42:18:51.3	-18.0±1.2 -30.0±1.0	9.58	0.74±0.04	G8Vq3	8.15±0.03 7.78±0.06 7.67±0.02	1RXS J155113.5-421858		
79610	UCL	16:14:43.02 -38:38:43.5	-14.1±3.4 -29.4±3.2	9.24	0.52±0.03	G1/G2Vq1	8.07±0.01 7.85±0.03 7.98±0.03	CCDM 16147-3839		
80636	UCL	16:27:52.34 -35:47:00.4	-13.1±2.1 -25.5±1.2	9.37	0.68±0.03	G6Vq2	8.04±0.01 7.71±0.01 7.62±0.01	1RXS J162752.8-354702		
81380	UCL	16:37:12.87 -39:00:38.1	-14.4±2.1 -21.5±1.6	9.82	0.66±0.05	G2/5Vq3	8.45±0.02 8.09±0.04 7.99±0.03	...		
81447	UCL	16:38:05.53 -34:01:10.6	-11.3±1.5 -23.9±1.0	9.08	0.54±0.05	G1IV/Vq1	7.91±0.02 7.66±0.03 7.55±0.03	...		
81775	UCL	16:42:10.36 -31:30:15.0	-14.1±1.5 -18.3±1.3	9.44	0.64±0.04	G5Vq2	8.36±0.02 8.37±0.05 8.08±0.04	...		

NOTE.— Columns: (1) *Hipparcos* ID, (2) OB subgroup region, (3) J2000.0 position, (4) proper motion components (mas yr⁻¹; where $\mu_{\alpha*} = \mu_{\alpha}\cos\delta$), (5) V magnitude (Johnson), (6) $B - V$ color (Johnson), (7) Spectral types from the Michigan Spectral Survey (Vol. 1-3); “q1” indicates the flag “quality = 1” in the MSS catalog, where q=1,2 stars are judged to have reliable spectral types, (8-10) 2MASS JHK_s magnitudes, (11) Notes on variability, X-ray counterparts, and multiple star system name (CCDM) from *Hipparcos*. “Var.(N.NN)” indicates that the H6 field in the *Hipparcos* catalog is identified as being variable in the broad H_p pass-band. The magnitude scatter N.NN in H_p is listed, and period P if found. Near-IR photometry is from the preliminary 2MASS database. The name is given of RASS-BSC X-ray sources within 40" of *Hipparcos* stars; many of the variable stars are also *ROSAT* sources. Astrometric data and optical photometry are from the *Hipparcos* catalog European Space Agency (1997).

TABLE 2
PROPERTIES OF RASS-ACT/TRC CANDIDATES

(1) Name TYC	(2) OB Grp.	(3) α, δ (J2000) h m s ° ' "	(4) $\mu_{\alpha*}, \mu_{\delta}$ (mas yr ⁻¹)	(5) V _T (mag)	(6) B _T - V _T (mag)	(7) J (mag)	(8) H (mag)	(9) K _s (mag)	(10) 1RXS Name	(11) sep. (")	(12) X-ray (ct s ⁻¹)	(13) Hrdns. HR1	(14) Table 5 #	
9212-2011-1	LCC	10:57:49.38 -69:13:59.9	-36.1±2.4	5.7±2.3	10.49±0.04	1.09±0.08	8.49±0.03	8.02±0.05	7.79±0.01	J105751.2-691402	10	1.61e-01	0.31	1
8625-388-1	LCC	11:32:08.34 -58:03:20.0	-41.6±3.1	-1.4±3.0	10.02±0.03	1.02±0.06	8.09±0.02	7.64±0.04	7.48±0.02	J113209.3-580319	7	8.25e-02	0.03	2
8222-105-1	LCC	11:35:03.76 -64:50:22.0	-24.7±2.0	-7.0±1.9	10.35±0.03	0.75±0.05	9.22±0.02	8.93±0.03	8.86±0.03	J113501.5-485011	24	1.01e-01	0.49	...
8982-3046-1	LCC	12:04:14.42 -64:18:51.7	-28.9±3.9	-4.7±3.7	10.09±0.03	0.75±0.05	8.82±0.01	8.50±0.02	8.40±0.02	J120413.3-641837	16	2.77e-01	0.32	...
8982-3213-1	LCC	12:04:48.87 -64:09:55.4	-32.9±3.5	+0.8±3.1	9.49±0.02	0.79±0.03	8.05±0.01	7.71±0.01	7.61±0.01	J120448.2-640942	13	3.47e-01	0.46	3
8640-2515-1	LCC	12:06:13.54 -57:02:16.8	-24.6±2.8	-7.7±2.6	10.77±0.05	0.81±0.08	9.25±0.03	8.84±0.03	8.77±0.03	J120613.9-570215	3	1.44e-01	0.27	4
8644-802-1	LCC	12:09:41.86 -58:54:45.0	-33.8±3.1	-11.8±2.8	10.21±0.03	1.26±0.07	8.31±0.01	7.81±0.01	7.66±0.01	J120941.5-585440	5	2.33e-01	0.16	5
8644-340-1	LCC	12:11:31.43 -58:16:53.2	-36.0±2.6	-8.7±1.8	10.29±0.04	1.00±0.07	8.58±0.01	8.09±0.03	7.96±0.02	J121131.9-581651	4	2.41e-01	0.09	6
9231-1566-1	LCC	12:11:38.14 -71:10:36.0	-38.9±1.4	-8.3±1.4	9.23±0.02	0.79±0.03	7.68±0.01	7.31±0.04	7.19±0.02	J121137.3-711032	5	2.68e-01	0.34	7
8636-2515-1	LCC	12:12:35.75 -55:20:27.3	-34.5±2.1	-13.4±2.3	10.58±0.04	1.11±0.08	8.73±0.02	8.25±0.03	8.13±0.02	J121236.4-552037	11	1.83e-01	-0.02	8
8242-1324-1	LCC	12:14:34.09 -51:10:12.5	-35.7±2.1	-12.9±1.9	10.38±0.03	1.05±0.06	8.69±0.01	8.26±0.04	8.13±0.02	J121434.2-511004	8	1.77e-01	0.32	9
8637-2610-1	LCC	12:14:52.31 -55:47:03.6	-38.3±3.6	-7.2±3.4	9.73±0.02	0.92±0.04	8.04±0.02	7.66±0.02	7.52±0.01	J121452.4-554704	0	5.65e-01	0.37	10
8645-1339-1	LCC	12:18:27.64 -59:43:12.9	-41.6±3.7	-1.9±3.3	10.82±0.05	0.95±0.09	8.45±0.01	7.84±0.01	7.73±0.01	J121828.6-594307	8	1.78e-01	0.39	11
8641-2187-1	LCC	12:18:58.02 -57:37:19.2	-36.5±1.8	-10.2±1.5	9.96±0.03	1.02±0.05	7.96±0.01	7.47±0.04	7.31±0.01	J121858.2-573713	5	2.93e-01	0.23	12
8983-98-1	LCC	12:19:21.64 -64:54:10.4	-37.0±3.0	-11.2±2.8	10.21±0.04	1.01±0.07	8.03±0.01	7.55±0.01	7.38±0.01	J121919.4-645406	14	2.55e-01	0.26	13
8633-508-1	LCC	12:21:16.48 -53:17:44.9	-36.8±1.9	-7.7±1.8	9.41±0.02	0.76±0.03	8.08±0.01	7.74±0.02	7.65±0.02	J122116.7-531747	3	4.34e-01	-0.03	14
8238-1462-1	LCC	12:21:55.65 -49:46:12.5	-37.4±1.5	-14.2±1.3	10.10±0.03	0.90±0.05	8.49±0.02	8.05±0.02	8.02±0.03	J122155.9-494609	3	1.13e-01	0.59	15
8234-2856-1	LCC	12:22:04.30 -48:41:24.9	-30.0±2.0	-12.1±1.9	10.59±0.04	0.95±0.06	8.78±0.02	8.27±0.03	8.17±0.01	J122204.0-484118	7	1.10e-01	0.88	16
8633-28-1	LCC	12:22:33.23 -53:33:49.0	-31.7±1.5	-7.7±1.5	9.49±0.02	0.72±0.03	8.18±0.01	7.91±0.04	7.78±0.02	J122233.4-533347	2	1.43e-01	0.00	17
8641-1281-1	LCC	12:23:40.13 -56:16:32.5	-33.1±3.3	-14.0±3.0	10.94±0.06	0.94±0.09	9.02±0.02	8.53±0.05	8.37±0.03	J122339.9-561628	4	8.03e-02	0.15	18
8992-605-1	LCC	12:36:38.97 -63:44:43.5	-37.8±2.0	-9.7±1.9	9.98±0.03	1.10±0.05	8.02±0.01	7.51±0.01	7.35±0.01	J123637.5-634446	10	2.17e-01	0.09	19
8646-166-1	LCC	12:36:58.97 -54:12:18.0	-32.3±3.3	-13.9±3.0	10.50±0.04	1.07±0.07	8.75±0.04	8.28±0.03	8.16±0.02	J123657.4-541217	13	1.06e-01	0.44	20
8654-1115-1	LCC	12:39:37.96 -57:31:40.7	-35.2±2.5	-21.9±2.4	10.21±0.03	0.88±0.05	8.67±0.01	8.23±0.04	8.13±0.03	J123938.4-573141	3	2.34e-01	0.33	21
8659-2604-1	LCC	12:41:18.17 -58:25:56.0	-37.7±2.5	-17.6±2.3	10.01±0.03	0.81±0.05	8.40±0.01	8.02±0.02	7.89±0.01	J124118.5-582556	2	1.19e-01	0.81	22
8992-420-1	LCC	12:44:34.82 -63:31:46.2	-31.2±3.3	-7.7±3.0	10.91±0.05	1.40±0.14	8.54±0.01	8.01±0.01	7.87±0.01	J124432.6-633139	16	2.11e-01	0.39	23
8249-52-1	LCC	12:45:06.76 -47:42:58.2	-31.2±1.3	-14.4±1.3	10.48±0.04	0.86±0.06	8.70±0.02	8.23±0.02	8.10±0.01	J124506.9-474254	4	2.22e-01	0.30	24
7783-1908-1	LCC	12:48:07.79 -44:39:16.8	-39.7±1.3	-18.0±1.3	9.82±0.03	0.93±0.05	8.12±0.01	7.69±0.05	7.51±0.02	J124807.6-443913	4	4.33e-01	0.05	25
8655-149-1	LCC	12:48:48.18 -56:35:37.8	-29.4±1.7	-9.4±1.7	10.31±0.03	0.92±0.05	8.88±0.01	8.48±0.02	8.39±0.02	J124847.4-563525	13	9.77e-02	0.77	26
9245-617-1	LCC	12:58:25.58 -70:28:49.2	-43.1±1.5	-18.7±1.5	10.01±0.03	0.98±0.06	8.20±0.02	7.70±0.06	7.56±0.02	J125824.6-702848	4	2.30e-01	0.11	27
8648-446-1	LCC	13:01:50.70 -53:04:58.3	-32.6±4.4	-19.5±4.0	11.18±0.06	1.02±0.13	9.44±0.02	8.91±0.02	8.78±0.02	J130153.7-530446	29	8.19e-02	0.12	28
8652-1791-1	LCC	13:02:37.54 -54:59:36.8	-25.5±2.0	-6.6±2.0	10.35±0.03	0.72±0.05	8.86±0.01	8.57±0.03	8.48±0.02	J130237.2-545933	4	1.59e-01	0.92	29
8258-1878-1	LCC	13:06:40.12 -51:59:38.6	-33.3±2.4	-15.7±2.2	10.62±0.04	0.91±0.07	8.90±0.01	8.44±0.04	8.27±0.01	J130638.5-515948	17	8.46e-02	0.58	30
8990-701-1	LCC	13:13:28.11 -60:00:44.6	-26.6±3.0	-5.3±2.8	10.08±0.02	0.70±0.04	8.76±0.01	8.45±0.02	8.42±0.02	J131327.3-600032	13	1.23e-01	0.36	...
8259-689-1	LCC	13:14:23.84 -50:54:01.9	-27.4±2.1	-16.4±1.9	10.48±0.04	0.96±0.08	8.68±0.03	8.27±0.03	8.10±0.04	J131424.3-505402	4	2.72e-01	0.41	31
8649-251-1	LCC	13:17:56.94 -53:17:56.2	-23.4±3.4	-8.3±3.2	10.48±0.05	0.72±0.08	8.86±0.03	8.49±0.05	8.39±0.03	J131754.9-531758	18	1.60e-01	0.36	32
8248-539-1	LCC	13:22:04.46 -45:03:23.1	-26.7±1.6	-13.3±1.4	10.10±0.03	0.77±0.06	8.97±0.03	8.63±0.05	8.55±0.03	J132204.7-450312	10	7.06e-02	0.53	33
9246-971-1	LCC	13:22:07.54 -69:38:12.3	-40.8±2.5	-23.0±2.3	10.54±0.04	1.08±0.08	8.28±0.03	7.65±0.02	7.31±0.01	J132207.2-693812	1	1.58e-01	0.59	34
8663-1375-1	LCC	13:34:20.26 -52:40:36.1	-33.4±1.6	-21.1±1.3	9.37±0.02	0.71±0.03	8.04±0.01	7.69±0.04	7.56±0.03	J133420.0-524032	4	2.51e-01	0.44	35
7796-1788-1	UCL	13:37:57.29 -41:34:41.9	-36.7±1.2	-24.2±1.2	10.17±0.04	0.97±0.06	8.47±0.01	8.03±0.04	7.89±0.02	J133758.0-413448	10	2.22e-01	0.27	36
8667-283-1	LCC	13:43:28.53 -54:36:43.5	-44.0±1.8	-20.8±1.8	9.39±0.02	0.77±0.03	8.03±0.01	7.68±0.01	7.63±0.02	J134332.7-543638	36	4.81e-01	0.22	37
8270-2015-1	UCL	13:47:50.55 -49:02:05.5	-24.3±2.2	-14.7±2.0	10.91±0.07	0.90±0.11	9.30±0.01	8.81±0.05	8.70±0.03	J134748.0-490158	26	1.50e-01	-0.10	38
8263-2453-1	UCL	13:52:47.80 -46:44:09.2	-22.7±1.3	-18.9±1.4	9.69±0.03	0.72±0.04	8.41±0.02	8.07±0.04	7.94±0.01	J135247.0-464412	8	1.96e-01	0.67	39
7811-2909-1	UCL	14:02:20.73 -41:44:50.8	-27.6±2.0	-19.4±1.9	10.80±0.06	0.90±0.10	8.99±0.02	8.55±0.04	8.42±0.03	J140220.9-414435	15	9.68e-02	0.37	40
7815-2029-1	UCL	14:09:03.58 -44:38:44.4	-20.9±1.1	-22.6±1.1	9.46±0.02	0.71±0.04	8.25±0.01	7.98±0.05	7.86±0.02	J140902.6-443838	12	1.73e-01	0.67	41
9244-814-1	LCC	14:16:05.67 -69:17:36.0	-29.4±2.4	-16.0±2.3	10.21±0.03	0.72±0.06	8.74±0.01	8.39±0.02	8.36±0.02	J141605.3-691756	20	6.10e-02	0.47	42
8285-847-1	UCL	14:16:57.91 -49:56:42.3	-23.2±1.1	-22.1±1.1	8.77±0.01	0.71±0.02	7.43±0.02	7.12±0.02	7.03±0.01	J141658.4-495648	7	1.59e-01	0.15	...
8282-516-1	UCL	14:27:05.56 -47:14:21.8	-25.5±1.7	-21.2±1.6	10.68±0.05	0.95±0.08	9.06±0.03	8.65±0.03	8.52±0.03	J142705.3-471420	3	1.53e-01	-0.12	43

TABLE 2—Continued

(1) Name TYC	(2) OB Grp.	(3) α, δ (J2000) h m s ° ' "	(4) $\mu_{\alpha*}$, μ_{δ} (mas yr ⁻¹)	(5) V _T (mag)	(6) $B_T - V_T$ (mag)	(7) J (mag)	(8) H (mag)	(9) K _s (mag)	(10) 1RXS Name	(11) sep. (")	(12) X-ray (ct s ⁻¹)	(13) Hrdns.	(14) Table 5 HR1 #
7817-622-1	UCL	14:28:09.30 -44:14:17.4	-18.4±2.0 -20.6±1.9	9.87±0.03	0.90±0.05	8.31±0.01	7.93±0.03	7.78±0.03	J142809.6-441438	20	1.45e-01	0.13	44
7813-224-1	UCL	14:28:19.38 -42:19:34.1	-19.7±1.5 -19.8±1.7	10.55±0.05	0.79±0.09	8.92±0.01	8.51±0.03	8.40±0.03	J142817.6-421958	31	2.23e-01	0.34	45
7814-1450-1	UCL	14:37:04.22 -41:45:03.0	-21.5±2.0 -19.1±1.9	9.77±0.02	0.72±0.04	8.26±0.01	7.90±0.02	7.80±0.03	J143704.6-414504	4	1.68e-01	0.58	46
8683-242-1	UCL	14:37:50.23 -54:57:41.1	-18.3±2.5 -25.8±2.4	10.80±0.06	0.77±0.09	8.94±0.01	8.46±0.02	8.32±0.02	J143750.9-545708	33	2.20e-01	0.07	47
8283-264-1	UCL	14:41:35.00 -47:00:28.8	-29.6±1.3 -27.4±1.2	10.09±0.03	0.88±0.04	8.43±0.01	7.98±0.03	7.88±0.03	J144135.3-470039	11	6.12e-01	0.15	48
8283-2795-1	UCL	14:47:31.77 -48:00:05.7	-29.6±2.3 -16.7±2.3	10.79±0.06	0.75±0.09	9.37±0.01	9.04±0.01	8.96±0.03	J144732.2-480019	14	7.37e-02	0.50	49
7305-380-1	UCL	14:50:25.81 -35:06:48.6	-18.2±2.6 -15.8±2.6	10.83±0.07	0.97±0.13	8.75±0.03	8.24±0.02	8.11±0.03	J145025.4-350645	6	9.03e-02	0.35	50
7828-2913-1	UCL	14:52:41.98 -41:41:55.2	-22.6±2.2 -21.4±2.1	11.02±0.09	1.35±0.22	9.05±0.02	8.40±0.02	8.29±0.03	J145240.7-414206	17	1.30e-01	0.21	51
7310-2431-1	UCL	14:57:19.63 -36:12:27.4	-26.6±1.6 -22.3±1.7	10.36±0.05	0.97±0.09	8.78±0.03	8.44±0.04	8.30±0.03	J145720.4-361242	17	8.67e-02	0.69	52
7310-503-1	UCL	14:58:37.70 -35:40:30.4	-21.4±2.2 -26.0±2.3	10.88±0.07	1.37±0.20	8.65±0.01	8.08±0.03	7.90±0.01	J145837.6-354036	5	8.30e-02	0.60	53
7824-1291-1	UCL	14:59:22.76 -40:13:12.1	-26.0±1.4 -26.5±1.6	9.80±0.04	0.86±0.07	8.34±0.01	7.97±0.04	7.82±0.02	J145923.0-401319	7	1.87e-01	0.35	54
7833-2037-1	UCL	15:00:51.88 -43:31:21.0	-20.1±2.1 -19.1±2.0	11.23±0.08	0.81±0.13	9.31±0.03	8.88±0.02	8.75±0.03	J150052.5-433107	15	7.57e-02	0.39	55
7829-504-1	UCL	15:01:11.56 -41:20:40.6	-14.9±1.7 -15.1±1.7	10.09±0.03	0.77±0.06	8.78±0.03	8.47±0.05	8.33±0.03	J150112.0-412040	4	1.78e-01	0.41	56
8297-1613-1	UCL	15:01:58.82 -47:55:46.4	-22.2±1.7 -18.2±1.6	10.22±0.04	0.71±0.07	8.91±0.01	8.59±0.02	8.51±0.02	J150158.5-475559	13	5.07e-02	0.42	57
7319-749-1	UCL	15:07:14.81 -35:04:59.6	-34.1±2.4 -30.1±2.5	10.59±0.06	1.00±0.11	8.87±0.01	8.42±0.05	8.35±0.03	J150714.5-350500	3	7.39e-02	0.71	58
7833-1106-1	UCL	15:08:00.55 -43:36:24.9	-21.8±1.4 -16.5±1.4	9.93±0.03	0.87±0.06	8.20±0.01	7.86±0.04	7.71±0.02	J150759.9-433642	18	8.84e-02	0.88	...
7833-2400-1	UCL	15:08:37.75 -44:23:16.9	-17.9±2.1 -17.6±2.0	10.91±0.07	0.80±0.11	9.33±0.03	8.95±0.02	8.81±0.03	J150836.0-442325	20	1.73e-01	0.45	59
7833-2559-1	UCL	15:08:38.50 -44:00:52.1	-23.5±2.1 -24.2±1.9	10.61±0.05	0.70±0.09	8.95±0.02	8.54±0.03	8.54±0.03	J150838.5-440048	4	1.21e-01	0.19	60
8293-92-1	UCL	15:09:27.93 -46:50:57.2	-19.9±2.1 -16.1±2.0	10.60±0.05	0.99±0.09	8.39±0.04	7.83±0.04	7.72±0.02	J150928.2-465109	12	7.77e-02	1.00	...
8294-2230-1	UCL	15:12:50.18 -45:08:04.5	-19.8±2.1 -22.4±2.0	10.79±0.07	0.85±0.11	9.13±0.01	8.74±0.03	8.67±0.02	J151250.0-450822	17	1.45e-01	0.19	61
8694-1685-1	UCL	15:18:01.74 -53:17:28.8	-28.7±2.5 -28.3±2.3	10.21±0.04	0.86±0.07	8.51±0.02	8.12±0.04	8.01±0.02	J151802.0-531719	10	2.23e-01	-0.04	62
7822-158-1	UCL	15:18:26.91 -37:38:02.1	-22.5±2.6 -28.3±2.6	11.11±0.09	0.87±0.15	9.07±0.03	8.63±0.04	8.53±0.03	J151827.3-373808	7	1.30e-01	0.37	63
8295-1530-1	UCL	15:25:59.65 -45:01:15.8	-21.9±2.2 -21.3±2.0	10.98±0.07	0.88±0.12	9.45±0.02	8.98±0.02	8.88±0.02	J152600.9-450113	13	6.10e-02	-0.15	64
7326-928-1	UCL	15:29:38.58 -35:46:51.3	-21.7±2.0 -26.1±2.1	10.54±0.06	1.07±0.11	8.77±0.01	8.27±0.03	8.19±0.03	J152937.7-354656	11	1.05e-01	0.21	65
7318-593-1	UCL	15:31:21.93 -33:29:39.5	-25.8±2.5 -31.5±2.5	10.99±0.08	0.72±0.12	9.39±0.03	8.95±0.06	8.81±0.03	J153121.8-333002	23	9.34e-02	0.06	...
7327-1934-1	UCL	15:37:02.14 -31:36:39.8	-17.8±1.6 -29.0±1.6	10.06±0.04	0.70±0.06	8.28±0.03	7.76±0.04	7.72±0.02	J153701.9-313647	7	3.92e-01	0.32	66
7840-1280-1	UCL	15:37:11.30 -40:15:56.8	-16.7±1.9 -22.5±1.9	10.55±0.05	1.24±0.10	8.98±0.01	8.46±0.05	8.31±0.03	J153711.6-401608	11	2.27e-01	-0.14	67
7848-1659-1	UCL	15:38:43.06 -44:11:47.4	-23.2±1.6 -28.4±1.5	10.36±0.05	0.85±0.08	8.81±0.05	8.36±0.04	8.22±0.03	J153843.1-441149	1	1.41e-01	-0.01	68
6785-510-1	UCL	15:39:24.41 -27:10:21.9	-20.2±1.7 -29.8±1.6	9.65±0.03	0.81±0.05	8.04±0.03	7.64±0.03	7.53±0.01	J153924.0-271035	14	2.33e-01	0.59	69
7331-782-1	UCL	15:44:03.77 -33:11:11.2	-22.2±2.6 -29.7±2.6	10.97±0.07	0.95±0.12	9.05±0.02	8.55±0.01	8.41±0.03	J154404.1-331120	10	7.72e-02	0.42	70
7845-1174-1	UCL	15:45:52.25 -42:22:16.5	-18.0±1.5 -30.4±1.6	10.61±0.05	1.15±0.09	8.69±0.02	8.09±0.04	7.94±0.02	J154552.7-422227	11	4.13e-01	0.07	71
8317-551-1	UCL	15:46:51.79 -49:19:04.7	-19.7±1.6 -27.9±1.5	10.29±0.04	0.94±0.08	8.69±0.01	8.36±0.03	8.31±0.02	J154651.5-491922	17	1.78e-01	0.07	72
7842-250-1	UCL	15:56:59.05 -39:33:43.1	-15.1±2.0 -21.6±2.0	10.90±0.07	0.94±0.12	9.20±0.02	8.83±0.03	8.70±0.03	J155659.0-393400	16	9.87e-02	-0.02	73
7333-1260-1	UCL	16:01:07.93 -32:54:52.5	-18.3±1.4 -29.6±1.5	9.58±0.02	0.73±0.04	8.46±0.01	8.16±0.04	8.08±0.02	J160108.0-325455	3	1.93e-01	0.34	74
7333-719-1	UCL	16:01:08.97 -33:20:14.2	-12.3±2.1 -23.0±2.2	10.99±0.07	1.15±0.16	9.01±0.02	8.55±0.03	8.46±0.03	J160108.9-332021	7	9.66e-02	0.75	75
7863-1629-1	UCL	16:03:45.37 -43:55:49.2	-12.5±1.1 -22.6±1.4	9.74±0.03	1.06±0.05	7.93±0.02	7.42±0.03	7.30±0.01	J160345.8-435544	6	4.09e-01	0.21	76
7855-1106-1	UCL	16:03:52.50 -39:39:01.3	-16.4±2.4 -28.4±2.3	11.12±0.08	1.15±0.18	8.98±0.03	8.35±0.03	8.21±0.03	J160352.0-393901	5	1.29e-01	-0.02	77
7851-1-1	UCL	16:05:45.00 -39:06:06.5	-16.8±2.2 -31.1±2.2	10.63±0.06	1.00±0.10	8.93±0.02	8.52±0.04	8.36±0.03	J160545.8-390559	11	1.57e-01	0.46	78
7355-317-1	UCL	16:13:58.02 -36:18:13.4	-18.4±2.0 -32.3±2.1	11.26±0.09	1.17±0.21	9.41±0.02	8.98±0.03	8.84±0.03	J161357.9-361813	1	1.74e-01	0.03	79
8319-1687-1	UCL	16:14:52.01 -50:26:18.5	-19.9±2.1 -29.2±2.0	10.50±0.05	0.96±0.09	8.38±0.01	7.91±0.01	7.76±0.01	J161451.3-502621	7	2.37e-01	0.15	80
7852-51-1	UCL	16:18:38.56 -38:39:11.8	-25.9±1.3 -34.0±1.5	9.09±0.02	0.69±0.03	8.02±0.01	7.79±0.05	7.69±0.02	J161839.0-383927	16	1.62e-01	-0.06	81
7857-648-1	UCL	16:21:12.19 -40:30:20.6	-9.1±1.4 -28.1±1.4	10.67±0.05	1.01±0.09	8.97±0.02	8.55±0.02	8.43±0.02	J162112.0-403032	11	1.29e-01	0.13	82
7857-514-1	UCL	16:23:29.55 -39:58:00.8	-12.5±2.1 -24.1±2.1	10.73±0.06	0.88±0.09	9.47±0.02	9.10±0.03	8.99±0.03	J162330.1-395806	8	7.93e-02	0.18	83
7853-227-1	UCL	16:27:30.55 -37:49:21.6	-10.0±2.5 -23.4±2.6	11.05±0.07	0.84±0.12	9.29±0.02	8.81±0.04	8.66±0.03	J162730.0-374929	9	6.24e-02	1.00	84
7353-2640-1	UCL	16:31:42.03 -35:05:17.2	-16.2±1.9 -27.6±2.0	10.72±0.05	0.81±0.08	9.19±0.02	8.75±0.02	8.63±0.02	J163143.7-350521	20	8.92e-02	0.52	85
7349-2191-1	UCL	16:35:35.99 -33:26:34.7	-6.0±1.8 -23.0±2.1	11.09±0.07	0.93±0.13	8.99±0.02	8.44±0.03	8.28±0.02	J163533.9-332631	25	1.65e-01	0.37	86
7858-526-1	UCL	16:38:38.47 -39:33:03.5	-10.4±1.3 -19.2±1.3	9.05±0.02	0.73±0.04	7.52±0.01	7.25±0.02	7.15±0.01	J163839.2-393307	9	8.45e-02	0.61	...

TABLE 2—Continued

(1) Name TYC	(2) OB Grp.	(3) α, δ (J2000) h m s ° ' "	(4) $\mu_{\alpha*}, \mu_{\delta}$ (mas yr ⁻¹)	(5) V_T (mag)	(6) $B_T - V_T$ (mag)	(7) J (mag)	(8) H (mag)	(9) K_s (mag)	(10) 1RXS Name	(11) sep. (")	(12) X-ray (ct s ⁻¹)	(13) Hrdns.	(14) HR1 #
7858-830-1	UCL	16:39:59.30 -39:24:59.2	-9.7±2.2 -18.9±2.2	10.68±0.08	0.84±0.12	8.67±0.02	8.26±0.04	8.12±0.02	J163958.7-392457	7	7.39e-02	0.96	87
7871-1282-1	UCL	16:42:24.00 -40:03:29.7	-11.1±1.5 -20.2±1.3	9.70±0.03	0.88±0.06	8.03±0.03	7.63±0.05	7.46±0.02	J164224.5-400329	5	9.83e-02	0.44	88

NOTE.— Columns: (1) Tycho-2 name, (2) OB subgroup region, (3) J2000.0 position from Tycho-2 catalog, (4) proper motion (α^*, δ components) in mas yr⁻¹ (where $\mu_{\alpha*} = \mu_{\alpha} \cos \delta$), (5) V_T magnitude, (6) $B - V_T$ color, (7-9) 2MASS JHK_s magnitudes, (10) X-ray counterpart name in RASS-BSC, (11) optical-X-ray separation, (12) X-ray count rate (ct s⁻¹), (13) Hardness ratio HR1, (14) Number in Table 5 if star is found to be “pre-MS” or “pre-MS?” in nature. X-ray data is from *ROSAT* All-Sky Survey BSC (Voges et al. 1999), astrometry and optical photometry are from *Tycho-2* catalog (Høg et al. 2000a), and near-IR photometry is from the 2MASS working database.

TABLE 3
SPECTRAL STANDARD STARS

Name HD	Name HR	MK Sp.Type	V (mag)	$\pi \pm \sigma_\pi$ (mas)	$B - V$ (mag)	[Fe/H] adopted	MSS Sp.Type	Adopted Sp.Type	notes ...
182640	7377	F0IV	3.36	65.1 ± 0.8	0.32	...	F2V	F0IV	^{a,b}
173677	7061	F6V	4.19	52.4 ± 0.7	0.48	-0.1	...	F6IV-V	^c
84117	3862	F9V	4.93	67.2 ± 0.7	0.53	...	G0V	F9V	
121370	5235	G0IV	2.68	88.2 ± 0.8	0.58	0.2	...	G0IV	^b
89010	4030	G1.5IV-V	5.95	32.9 ± 0.9	0.66	0.0	...	G1.5IV-V	
126868	5409	G2IV	4.84	24.2 ± 1.0	0.69	0.0	G3V	G2III-IV	^{a,d}
161239	6608	G2IIIb	5.73	26.1 ± 0.6	0.68	G2IV	
146233	6060	G2Va	5.49	71.3 ± 0.9	0.65	0.0	G5V	G2V	^a
94481	4255	G4III	5.65	8.0 ± 0.8	0.83	...	K0III+(G)	G4III	
117176	5072	G4V	4.97	55.2 ± 0.7	0.71	-0.1	...	G4IV-V	^e
188376	7597	G5IV	4.70	42.0 ± 0.9	0.75	-0.1	G3/5III	G5IV	^f
115617	5019	G6.5V	4.74	117.3 ± 0.7	0.71	0.0	G5V	G6.5V	
114946	4995	G7IV-V	5.31	25.9 ± 0.7	0.86	-0.1:	G8III/IV	G7IV	
188512	7602	G8IV	3.71	73.0 ± 0.8	0.86	0.0:	...	G8IV	^a
165760	6770	G8III	4.64	13.7 ± 0.8	0.95	-0.1	...	G8III	
95272	4287	K0+III	4.08	18.7 ± 1.0	1.08	-0.1:	K1III	K0+III	
131511	5553	K0.5V	6.00	86.7 ± 0.8	0.84	K0.5V	^a
165438	6756	K1IV	5.74	28.6 ± 0.8	0.97	0.0	K0IV	K1IV	
131977	5568	K4V	5.72	169.3 ± 1.7	1.02	0.0	K4V	K4V	
120467	...	K6Va	8.16	70.5 ± 1.0	1.26	K6V	

NOTE.— SB1,2 = spectroscopic binary in either SIMBAD or Duquennoy & Mayor (1991). MSS = Michigan Spectral Survey Vols. 1-5 = Houk & Cowley (1975), Houk (1978), Houk (1982), Houk & Smith-Moore (1988), Houk & Swift (1999). The [Fe/H] estimate is adopted from the compilation of published values in Cayrel de Strobel et al. (2001). A semi-colon after the [Fe/H] value indicates considerable scatter (>0.2 dex) in the published estimates.

^aSIMBAD lists as variable or suspected var., however *Hipparcos* finds scatter in $Hp \leq 0.015$ mag. The typical scatter for the other standard stars was 0.005 mag in Hp (*Hipparcos* magnitude), with none greater than 0.01 mag.

^bSpectroscopic binary

^cFrom standard list of Garcia (1989), and originally in Johnson & Morgan (1953), but not listed in either Keenan & Yorka (1988) or Keenan & McNeil (1989).

^dHR 5409 is a resolved binary (sep. 5") listed by SIMBAD as a variable star, however *Hipparcos* found the scatter in the Hp band to be only 0.015 mag.

^eHR 5072 is the planet host 70 Vir. Keenan & McNeil (1989) call it G4V, however it is G5V in virtually every other reference (e.g. Gray, Graham, & Hoyt (2001)). We retain Keenan's classification.

^f*Hipparcos* "G" binary

TABLE 4
STELLAR CLASSIFICATION SCHEME

Li-Rich	H α Excess	Lum. Class	N(R-T)	N(HIP)	Adopted Class.
			#	#	
Yes	Yes	IV	94	7	Pre-main sequence (PMS)
Yes	No	IV	3	6	Probably pre-main sequence? (PMS?)
Yes	Strong	IV	1	0	Pre-MS Classical T Tauri star (CTTS) ^a
Yes	Yes/No	V	4	1	Young Dwarf (ZAMS)
No	Yes	V	1	0	Active Dwarf
No	Yes	IV	4	0	Active Subgiant
No	No	IV	1	2	Subgiant
No	No	III	0	2	Giant
No	No	V	0	2	Dwarf (MS)
No	No(Wide)	IV	2	0	Chromosph.-Active Binary (CAB) ^b
...	107	20	Total

NOTE.—N(R-T) is number in RASS-ACT/TRC sample. N(HIP) is number in *Hipparcos* sample. “Li-rich” implies significant Li absorption, and above the line in Fig. 3. “Active” means that the H α equivalent widths are $>2 \times$ the σ -residual above the regression of values for field, standard stars (Fig. 2; Appendix C), implying that chromospheric emission is filling in the absorption line. Luminosity classes are assigned according to a star’s placement in Fig. 1.

^aincluded in Pre-MS sample count.

^bincluded in subgiant sample count.

TABLE 5
LCC & UCL PRE-MAIN SEQUENCE MEMBERS FROM DE ZEEUW ET AL. (1999) LIST

(1) Name HIP #	(2) OB Grp	(3) α, δ (J2000) h m s d ' ''	(4) π_{HIP} (mas)	(5) π_{sec} (mas)	(6) P ₁ %	(7) P ₃ %	(8) Spec. Type	(9) $\log(T_{eff})$ (K)	(10) $\log L/L_{\odot}$ (dex)	(11) A _V (mag)	(12) EW(H α) (Å)	(13) EW(Li) (Å)	(14) $\log(L_X)$ (erg s $^{-1}$)	(15) $\log(L_X /$ L _{bol})	(16) DM97 age, mass age
57524	LCC	11:47:24.55 -49:53:03.0	9.62 \pm 1.39	8.83 \pm 0.60	81	97	F9IV	3.783 \pm 0.004	0.44 \pm 0.06	0.30 \pm 0.10	2.0	0.18	30.8	-3.3	16 1.3
58996	LCC	12:05:47.48 -51:00:12.1	9.78 \pm 1.16	9.79 \pm 0.52	91	99	G1IV	3.772 \pm 0.005	0.43 \pm 0.05	0.14 \pm 0.04	3.3	0.21	30.5	-3.6	14 1.3
59854	LCC	12:16:27.84 -50:08:35.8	8.24 \pm 1.78	7.67 \pm 0.61	99	100	G1IV	3.772 \pm 0.006	0.49 \pm 0.07	0.37 \pm 0.11	1.6	0.20	30.9	-3.2	13 1.4
60885	LCC	12:28:40.05 -55:27:19.3	7.06 \pm 1.13	9.49 \pm 0.52	14	78	G0IV	3.778 \pm 0.005	0.46 \pm 0.05	0.16 \pm 0.05	2.7	0.13	30.3	-3.8	14 1.3
60913	LCC	12:29:02.25 -64:55:00.6	10.48 \pm 1.12	9.82 \pm 0.55	100	100	G4.5IV	3.758 \pm 0.008	0.43 \pm 0.05	0.21 \pm 0.04	2.0	0.19	<29.7	<-4.3	11 1.4
62445	LCC	12:47:51.87 -51:26:38.1	6.61 \pm 1.54	7.70 \pm 0.55	13	75	G4.5IV ^e	3.758 \pm 0.013	0.62 \pm 0.06	0.66 \pm 0.06	-1.8	0.24	30.7	-3.4	7 1.6
63847	LCC	13:05:05.29 -64:13:55.3	9.56 \pm 1.35	10.18 \pm 0.61	48	89	G3IV	3.764 \pm 0.007	0.36 \pm 0.06	0.33 \pm 0.06	1.6	0.22	<29.7	<-4.3	14 1.3
65517	LCC	13:25:45.81 -48:14:57.9	9.58 \pm 1.44	11.56 \pm 1.57	51	91	G2.5IV	3.770 \pm 0.005	0.02 \pm 0.05	0.14 \pm 0.04	1.9	0.17	30.4	-3.3	15 1.0
66001	LCC	13:30:53.11 -48:11:11	9.59 \pm 0.92	7.68 \pm 0.51	82	97	G2.5IV	3.770 \pm 0.011	0.50 \pm 0.07	0.10 \pm 0.10	1.2	0.18	30.6	-3.2	15 1.2
66941	LCC	13:43:08.69 -69:07:39.5	8.05 \pm 0.95	9.37 \pm 0.52	97	100	G0.5IV	3.775 \pm 0.008	1.09 \pm 0.05	0.38 \pm 0.04	2.1	0.16	31.1	3	2.4
67522	UCL	13:50:08.28 -40:50:08.8	7.94 \pm 1.64	7.91 \pm 0.60	93	99	G0.5IV	3.775 \pm 0.006	0.25 \pm 0.07	0.02 \pm 0.10	2.2	0.15	30.4	-3.5	20 1.2
71178	UCL	14:33:25.78 -34:32:37.6	9.76 \pm 1.90	8.71 \pm 0.56	99	100	G8IV ^e	3.741 \pm 0.012	0.16 \pm 0.06	0.35 \pm 0.08	-0.2	0.26	<29.8	<-3.9	14 1.2
75924	UCL	15:30:26.29 -32:18:11.6	10.91 \pm 3.21	9.79 \pm 0.79	16	57	G2.5IV	3.765 \pm 0.006	0.69 \pm 0.07	0.37 \pm 0.07	1.3	0.24	30.9	-2.9	7 1.6
76472	UCL	15:37:04.66 -40:09:22.1	5.70 \pm 1.63	7.24 \pm 0.49	95	99	G1IV	3.774 \pm 0.008	0.60 \pm 0.06	0.29 \pm 0.10	0.4	0.24	30.8	-3.3	11 1.4
77081	UCL	15:44:21.05 -33:18:55.0	6.63 \pm 1.61	7.66 \pm 0.59	69	92	G7.5IV	3.742 \pm 0.008	0.35 \pm 0.07	0.15 \pm 0.06	1.8	0.25	<29.9	<-4.1	9 1.4
77135	UCL	15:44:57.69 -34:11:53.7	6.98 \pm 2.92	7.20 \pm 0.98	91	96	G4IV	3.760 \pm 0.006	0.42 \pm 0.12	0.08 \pm 0.05	2.2	0.23	30.5	-3.4	12 1.4
77144	UCL	15:45:01.83 -40:50:31.0	6.45 \pm 1.42	8.00 \pm 0.53	43	86	G0IV	3.778 \pm 0.007	0.36 \pm 0.06	0.08 \pm 0.05	1.8	0.17	30.6	-3.4	17 1.2
77524	UCL	15:49:44.98 -39:25:09.1	6.63 \pm 1.93	6.63 \pm 0.76	96	99	K1-IV ^e	3.705 \pm 0.013	0.23 \pm 0.10	-0.03 \pm 0.10	-0.2	0.32	30.5	-3.3	4 1.4
77656	UCL	15:51:13.73 -42:18:51.3	6.52 \pm 1.37	7.70 \pm 0.52	100	100	G5IV	3.756 \pm 0.009	0.41 \pm 0.06	0.52 \pm 0.09	1.7	0.30	30.3	-3.8	11 1.4
80936	UCL	16:27:53.34 -33:00:04	8.24 \pm 1.04	9.60 \pm 0.52	33	82	G6.5IV	3.777 \pm 0.007	0.69 \pm 0.07	0.36 \pm 0.08	1.5	0.21	30.9	-3.3	10 1.5
81380	UCL	16:37:12.28 -39:00:08.1	7.24 \pm 1.91	9.92 \pm 0.53	32	99	G0IV	3.777 \pm 0.009	0.74 \pm 0.10	0.33 \pm 0.09	2.5	0.14	<30.3	9 1.6	
81447	UCL	16:38:05.53 -34:01:10.6	5.90 \pm 1.41	5.80 \pm 0.52	87	97	G0.5IV	3.775 \pm 0.005	0.78 \pm 0.08	0.03 \pm 0.07	2.8	0.13	<30.2	<-4.3	8 1.6

NOTE.— Columns: (1) *Hipparcos* catalog ID, (2) OB subgroup, (3) J2000.0 position, (4) *Hipparcos* astrometric parallax (mas), (5) Kinematic parallax estimate (mas) (see §6.3), (6) Membership probability (with v_{disp} = km s $^{-1}$), (8) Spectral type (see §4.1), (9) Effective temperature (see §6.2), (10) Luminosity (see §6.4), (11) Extinction A_V (see §6.4), (12) Equivalent Width of H α λ 6562.8 (Å), (13) Corrected EW of Li I λ 6707.8 (Å) upper limits assume RASS PSPC detection limit of 0.05 ct s $^{-1}$ and HR1 = 0), (15) Logarithm of ratio between X-ray and bolometric luminosities, (16) Age (in Myr) and Mass (in M/M $_{\odot}$) using DM97 tracks, (17) (18) Age (in Myr) and Mass (in M/M $_{\odot}$) using SDF00 tracks, (19) Class – PMS = pre-main sequence, PMS? = pre-main sequence? (see §5.1), (20) Notes – SB = spectroscopic binary.

^aHIP 59854 = CCDM J12165-5009AB. Unresolved binary ($\rho = 0.2''$).

^bHIP 65517. The Michigan Spectral Survey (Houk 1978) classifies this star as K0/2(V)+(G) (quality = 3). We found it to be much earlier (G1.5), and note that the published $b - y$ and $B - V$ colors support an

^cHIP 66941 = HD 119022 = Star "E" of Soderblom et al.'s (1998) high resolution survey of active southern stars. It is the most Li-rich of the very active stars in the Soderblom sample. We did not resolve this tight, e

^dHIP 75924 = CCDM J15304-3218AB. Both stars were on the slit ($\rho = 1.5''$).

^eHIP 77135 = [KWS97] Lupus 1 26 = CCDM J15450-3412AB. Binary is resolved ($\rho = 3.4''$) but both were on-slit.

^fHIP 77524 = [KWS97] TTS 79 = CCDM J15450-3412AB. Unresolved binary ($\rho = 0.2''$).

TABLE 6
PRE-MAIN SEQUENCE LCC & UCL RASS-ACT/TRC MEMBERS

(1) ID	(2) Name	(3) OB	(4) α, δ (J2000)	(5) π_{sec}	(6) P_1	(7) P_3	(8) Spec.	(9) $\log(T_{eff})$	(10) $\log L/L_\odot$	(11) A_V	(12) EW(H α)	(13) EW(Li)	(14) $\log(L_X)$	(15) $\log(L_X)/$	(16) DM97	F
#	TYC	Grp	h m s d '''	(mas)	%	%	Type	(K)	(dex)	(mag)	(Å)	(Å)	(erg s $^{-1}$)	L $_{bol}$	age, mass	age,n
1	9212-2011-1	LCC	10:57:49.38 -69:13:59.9	9.76 \pm 1.01	29	94	K1+IV	3.699 \pm 0.010	0.02 \pm 0.09	0.35 \pm 0.06	0.7	0.34	30.3	-3.3	7 1.2	13
2	8625-388-1	LCC	11:32:08.34 -58:03:20.0	10.78 \pm 1.21	59	84	G7IV	3.747 \pm 0.013	0.19 \pm 0.10	0.68 \pm 0.13	0.4	0.45	29.9	-3.7	15 1.2	19
3	8982-3213-1	LCC	12:04:48.87 -64:09:55.4	8.36 \pm 1.27	12	49	G4IV	3.773 \pm 0.005	0.44 \pm 0.13	0.60 \pm 0.11	1.5	0.21	30.8	-3.2	14 1.3	13
4	8640-2515-1	LCC	12:06:13.54 -57:02:16.8	6.48 \pm 1.06	90	97	G4IV	3.760 \pm 0.007	0.15 \pm 0.14	1.45 \pm 0.06	0.6	0.23	30.6	-3.2	27 1.1	25
5	8639-192-1	LCC	12:08:19.02 -57:00:09	9.41 \pm 0.54	65	88	K0IVe	3.770 \pm 0.013	0.18 \pm 0.11	0.28 \pm 0.10	-0.1	0.33	30.5	-3.2	7 1.2	12
6	8644-340-1	LCC	12:11:31.42 -58:16:53.2	9.29 \pm 0.91	95	99	G9IV	3.729 \pm 0.008	0.05 \pm 0.09	0.28 \pm 0.10	0.3	0.1	30.5	-3.2	7 1.2	21
7	9231-1566-1	LCC	12:11:38.48 -71:10:36.0	10.15 \pm 0.68	91	98	G3.5IV	3.762 \pm 0.005	0.39 \pm 0.06	0.48 \pm 0.08	1.4	0.27	30.5	-3.5	13 1.3	13
8	8636-2515-1	LCC	12:12:35.75 -55:20:27.3	9.24 \pm 0.90	50	84	K0+IV	3.717 \pm 0.007	0.00 \pm 0.09	0.48 \pm 0.12	0.2	0.34	30.3	-3.2	11 1.2	19
9	8242-1324-1	LCC	12:14:34.09 -51:10:12.5	9.41 \pm 0.83	82	96	G9IV	3.733 \pm 0.008	0.01 \pm 0.08	-0.02 \pm 0.05	0.2	0.33	30.4	-3.2	17 1.1	25
10	8637-2610-1	LCC	12:14:52.31 -55:47:03.6	9.72 \pm 1.31	62	84	G6IV	3.750 \pm 0.007	0.28 \pm 0.12	0.87 \pm 0.12	0.6	0.27	30.9	-2.9	13 1.3	15
11	8638-3339-1	LCC	12:18:27.02 -59:43:12.9	10.42 \pm 1.32	32	82	K0IVe	3.665 \pm 0.010	0.14 \pm 0.11	0.14 \pm 0.08	-0.3	0.30	30.3	-3.1	6 1.2	12
12	8641-2177-1	LCC	12:19:02.02 -57:01:19.2	9.14 \pm 0.74	97	99	G9.5IV	3.722 \pm 0.013	0.32 \pm 0.07	0.49 \pm 0.14	1.1	0.35	30.6	-3.2	6 1.5	10
13	8638-98-1	LCC	12:19:21.64 -64:54:10.4	9.74 \pm 1.13	89	97	K1-IV	3.707 \pm 0.010	0.26 \pm 0.10	0.25 \pm 0.05	0.3	0.32	30.6	-3.2	4 1.5	8
14	8633-508-1	LCC	12:21:16.48 -53:17:44.9	9.31 \pm 0.78	27	77	G1.5IV	3.770 \pm 0.007	0.31 \pm 0.07	0.44 \pm 0.07	1.6	0.21	30.7	-3.3	17 1.2	20
15	8238-1462-1	LCC	12:21:55.65 -49:46:12.5	9.85 \pm 0.66	86	98	G5.5IV	3.754 \pm 0.007	0.08 \pm 0.06	0.14 \pm 0.06	1.5	0.28	30.2	-3.4	22 1.1	28
16	8234-2856-1	LCC	12:22:04.30 -48:52:24.9	7.96 \pm 0.81	85	97	K0IVe	3.721 \pm 0.002	0.19 \pm 0.09	0.21 \pm 0.07	-0.1	0.34	30.4	-3.2	10 1.3	15
17	8637-2508-1	LCC	12:23:40.33 -59:33:09.0	8.03 \pm 0.69	53	89	G9IV	3.744 \pm 0.005	0.18 \pm 0.08	0.20 \pm 0.11	2.2	0.30	30.3	-3.3	16 1.2	17
18	8641-1281-1	LCC	12:23:40.13 -56:16:32.5	8.92 \pm 1.19	66	87	K0+IV	3.715 \pm 0.017	-0.09 \pm 0.12	0.44 \pm 0.09	1.1	0.36	30.0	-3.4	14 1.1	24
19	8992-605-1	LCC	12:36:38.97 -63:44:43.5	9.73 \pm 0.82	56	88	K0+III	3.717 \pm 0.017	0.25 \pm 0.08	0.39 \pm 0.06	0.6	0.37	30.4	-3.4	5 1.5	10
20	8646-166-1	LCC	12:36:58.97 -54:12:18.0	8.64 \pm 1.18	92	97	K0IV	3.721 \pm 0.006	0.04 \pm 0.12	0.11 \pm 0.05	0.7	0.32	30.3	-3.4	11 1.2	18
21	8654-1115-1	LCC	12:39:37.97 -56:31:40.7	10.22 \pm 0.96	3	39	G7.5IV	3.742 \pm 0.012	-0.06 \pm 0.08	0.30 \pm 0.07	0.1	0.26	30.4	-3.1	24 1.0	34
22	8659-2604-1	LCC	12:41:18.17 -58:25:56.0	10.26 \pm 0.95	58	87	G1.5IV	3.771 \pm 0.011	0.14 \pm 0.08	0.67 \pm 0.14	-0.6	0.29	30.2	-3.4	24 1.1	30
23	8992-420-1	LCC	12:44:34.82 -63:31:46.2	7.97 \pm 1.19	59	84	K1IVe	3.704 \pm 0.012	0.25 \pm 0.13	0.27 \pm 0.08	-0.7	0.38	30.6	-3.0	4 1.4	8
24	8249-52-1	LCC	12:45:06.76 -47:42:58.2	8.34 \pm 0.62	94	99	G8.5IV	3.738 \pm 0.011	0.13 \pm 0.07	0.38 \pm 0.14	0.0	0.30	30.6	-3.1	14 1.2	19
25	7732-9008-1	LCC	12:48:08.74 -53:33:33.1	7.98 \pm 0.75	25	75	G6IV	3.715 \pm 0.008	0.15 \pm 0.08	0.22 \pm 0.11	1.0	0.15	30.3	-3.5	26 1.2	30
26	8655-149-1	LCC	12:48:45.18 -56:35:37.8	7.56 \pm 0.73	56	89	K0+IV	3.715 \pm 0.017	0.14 \pm 0.09	0.53 \pm 0.13	1.2	0.22	30.4	-3.4	20 1.1	24
27	9245-817-1	LCC	12:58:28.59 -70:23:49.2	11.73 \pm 0.69	80	90	K0+IV	3.714 \pm 0.010	-0.04 \pm 0.08	0.49 \pm 0.12	0.0	0.37	30.3	-3.3	11 1.2	18
28	8643-446-1	LCC	12:59:50.70 -54:04:58.3	9.25 \pm 0.51	75	88	K2-IV	3.690 \pm 0.008	-0.37 \pm 0.14	0.50 \pm 0.10	0.2	0.33	30.0	-3.3	19 0.9	39
29	8652-1791-1	LCC	13:02:37.54 -54:59:36.8	6.40 \pm 0.81	16	67	G4IV	3.772 \pm 0.006	0.35 \pm 0.11	0.38 \pm 0.05	2.1	0.17	30.8	-3.1	16 1.2	18
30	8258-1878-1	LCC	13:06:40.12 -51:59:38.6	8.91 \pm 0.90	94	95	K0IVe	3.722 \pm 0.019	-0.05 \pm 0.09	0.17 \pm 0.09	-0.3	0.34	30.2	-3.4	15 1.1	24
31	8259-689-1	LCC	13:14:23.84 -50:54:01.9	7.70 \pm 0.81	87	97	G5.5IV	3.754 \pm 0.010	0.25 \pm 0.10	0.27 \pm 0.09	1.1	0.32	30.8	-2.9	15 1.2	18
32	8645-239-1	LCC	13:15:22.92 -54:55:52.9	7.59 \pm 0.51	56	81	G1.5IV	3.770 \pm 0.006	0.18 \pm 0.08	0.22 \pm 0.08	2.1	0.15	30.7	-3.5	26 1.2	30
33	8248-391-1	LCC	13:19:04.46 -45:03:33.1	7.61 \pm 0.67	74	94	K1IVe	3.702 \pm 0.017	0.00 \pm 0.08	0.17 \pm 0.07	-39.9	0.37	30.2	-3.2	8 1.2	14
34	9246-971-1	LCC	13:22:07.54 -69:38:12.3	11.57 \pm 0.95	82	95	K1IVe	3.702 \pm 0.017	0.00 \pm 0.08	0.17 \pm 0.07	-39.9	0.37	30.2	-3.2	8 1.2	14
35	8663-1375-1	LCC	13:34:20.26 -52:40:36.1	9.50 \pm 0.66	100	100	G4IV	3.774 \pm 0.007	0.32 \pm 0.06	0.45 \pm 0.10	1.7	0.22	30.5	-3.4	18 1.2	21
36	7796-1788-1	UCL	13:37:57.29 -41:34:41.9	10.23 \pm 0.52	49	88	K0IV	3.723 \pm 0.007	0.00 \pm 0.05	-0.07 \pm 0.05	0.7	0.30	30.4	-3.2	14 1.2	21
37	8667-283-1	LCC	13:43:23.53 -54:36:43.5	11.70 \pm 0.75	2	45	G8IVe	3.769 \pm 0.007	0.13 \pm 0.06	0.28 \pm 0.12	1.7	0.20	30.6	-3.2	24 1.1	30
38	8270-2015-1	UCL	13:47:50.55 -49:02:05.5	6.75 \pm 0.79	73	92	G8IVe	3.740 \pm 0.008	0.05 \pm 0.10	0.45 \pm 0.13	-0.5	0.29	30.5	-3.2	18 1.1	25
39	8269-457-1	UCL	13:50:24.01 -52:40:22.2	6.93 \pm 0.57	57	95	G9IV	3.743 \pm 0.008	0.07 \pm 0.08	0.21 \pm 0.08	2.4	0.18	30.8	-3.3	15 1.2	21
40	8111-2909-1	UCL	14:02:20.73 -44:44:50.8	6.76 \pm 0.71	58	87	G9IV	3.743 \pm 0.013	0.07 \pm 0.08	0.90 \pm 0.12	2.2	0.23	30.5	-3.3	14 1.2	21
41	7815-2029-1	UCL	14:09:03:58 -44:38:44.4	7.05 \pm 0.49	9	67	G9IV	3.783 \pm 0.005	0.50 \pm 0.06	0.38 \pm 0.06	3.0	0.11	30.7	-3.5	14 1.3	13
42	9244-814-1	LCC	14:16:05.47 -69:17:36.0	8.15 \pm 0.92	11	57	G11V	3.773 \pm 0.007	0.19 \pm 0.10	0.62 \pm 0.08	2.2	0.13	30.1	-3.7	23 1.1	27
43	8282-516-1	UCL	14:27:05.07 -47:41:21.8	7.57 \pm 0.63	89	98	G7.5IV	3.745 \pm 0.010	0.06 \pm 0.08	0.54 \pm 0.10	1.1	0.26	30.4	-3.3	19 1.1	26
44	7817-622-1	UCL	14:28:09.30 -44:41:57.4	6.23 \pm 0.71	52	85	G3.5IV	3.754 \pm 0.008	0.23 \pm 0.11	0.33 \pm 0.07	1.4	0.22	30.6	-3.5	8 1.5	16
45	7813-221-1	UCL	14:28:19.38 -42:19:34.1	6.27 \pm 0.61	87	97	G9.5IV	3.727 \pm 0.011	-0.12 \pm 0.08	0.44 \pm 0.10	1.2	0.25	30.0	-3.4	15 1.2	17
46	7844-1450-1	UCL	14:37:11.50 -41:45:04.6	6.41 \pm 0.70	88	97	G4.5IV	3.745 \pm 0.008	0.08 \pm 0.11	0.38 \pm 0.06	1.5	0.17	30.6	-3.4	11 1.4	14
47	8683-264-1	UCL	14:41:35:00 -47:00:28.8	9.11 \pm 0.52	94	99	G4IV	3.759 \pm 0.013	0.20 \pm 0.06	0.02 \pm 0.07	1.2	0.23	30.9	-3.0	18 1.2	24
48	8283-2795-1	UCL	14:47:31.77 -48:00:05.7	7.68 \pm 0.81	1	21	G2.5IV	3.766 \pm 0.008	-0.05 \pm 0.09	0.43 \pm 0.07	1.8	0.17	30.2	-3.		

TABLE 7
RASS-ACT/TRC & *Hipparcos* STARS REJECTED AS SCO-CEN MEMBERS

(1) Name	(2) α, δ (J2000) h m s d '''	(3) P ₁ %	(4) P ₃ %	(5) SpT ...	(6) EW(H α) (Å)	(7) EW(Li) (Å)	(8) $\log(L_X / L_{bol})$	(9) Type ...
TYC 8222-105-1	11:35:03.76 -48:50:22.0	71	93	F8.5V	2.7	0.19	-3.4	ZAMS
TYC 8982-3046-1	12:04:14.42 -64:18:51.7	97	99	G1V	2.0	0.20	-3.1	ZAMS
TYC 8990-701-1	13:13:28.11 -60:00:44.6	9	48	F9V	2.2	0.11	-3.4	ZAMS
TYC 8285-847-1	14:16:57.91 -49:56:42.3	43	87	G2.5IV	2.2	0.00	-3.9	subgiant (CAB)
TYC 7833-1106-1	15:08:00.55 -43:36:24.9	4	53	G2IV	0.6	0.00	-3.5	active subgiant
TYC 8293-92-1	15:09:27.93 -46:50:57.2	28	71	K0IV	0.7	0.05	-3.4	active subgiant
TYC 7318-593-1	15:31:21.93 -33:29:39.5	94	98	G9.5V	0.0	0.15	-3.3	active dwarf
TYC 7858-526-1	16:38:38.47 -39:33:03.5	98	100	F8.5IV	2.5	0.02	-4.0	active subgiant (CAB)
HIP 63797	13:04:30.96 -65:55:18.5	9	73	G3.5IV	2.4	0.00	<-4.5	subgiant
HIP 65423	13:24:35.12 -55:57:24.2	99	100	G0V	2.1	0.18	-3.6	ZAMS ^a
HIP 68726	14:04:07.12 -37:15:50.5	60	93	G0.5III	1.9	0.00	<-5.1	giant
HIP 72070	14:44:30.96 -39:59:20.6	62	91	G1V	2.6	0.16	<-4.2	ZAMS
HIP 74501	15:13:29.22 -55:43:54.6	3	61	G1.5III	2.4	0.03	<-4.9	giant
HIP 77015	15:43:29.86 -38:57:38.6	61	91	G0.5V	2.8	0.06	<-4.1	dwarf
HIP 79610	16:14:43.02 -38:38:43.5	37	74	G0.5V	2.7	0.03	<-4.2	dwarf
HIP 81775	16:42:10.36 -31:30:15.0	14	67	G1IV	2.8	0.04	<-4.1	subgiant

NOTE.— Columns: (1) Name from Tycho-2 or *Hipparcos* catalogs, (2) J2000.0 position, (3) Membership probability (with $v_{disp} = 1 \text{ km s}^{-1}$), (4) Membership probability (with $v_{disp} = 3 \text{ km s}^{-1}$), (5) Spectral type (see §4.1), (6) Equivalent width of H α $\lambda 6562.8 \text{ \AA}$, (7) Corrected EW of Li I $\lambda 6707.8 \text{ \AA}$, (8) Logarithm of ratio between X-ray and bolometric luminosities (approximate upper limits assume RASS PSPC detection limit of 0.05 ct s^{-1} and HR1 = 0), (9) Class of object

^aHIP 65423 = HD 116402. Cutispoto et al. (2002) measure EW(Li) = 220 m \AA , and $v\sin i = 35 \text{ km s}^{-1}$.

TABLE 8
AGE ESTIMATES OF LCC & UCL

Ref.	Tracks	method	age(LCC)	age(UCL)
			(Myr)	(Myr)
1	4	pre-MS	17 ± 1	15 ± 1
1	5	pre-MS	21 ± 2	19 ± 1
1	6	pre-MS	23 ± 2	22 ± 1
1	7	turn-off	16 ± 1	17 ± 1
2	8	turn-off	11-12	14-15
3	8,9	turn-off	10-11	12-13

NOTE.—Uncertainties are standard errors of the mean. Pre-MS age estimates exclude known SBs and stars with $\log T_{eff} < 3.73$, which bias the calculated ages. The turn-off ages from this work are determined using only early-B stars classified as members by de Zeeuw et al. (1999).

REFERENCES.—(1) this work, (2) de Geus et al. (1989), (3) de Zeeuw & Brand (1985), (4) D'Antona & Mazzitelli (1997), (5) Palla & Stahler (2001), (6) Siess, Dufour, & Forestini (2000), (7) Bertelli et al. (1994), (8) Maeder (1981), (9) Cogan (priv. comm.)

TABLE 9
REVISED LUMINOSITY CLASSES OF STANDARD STARS

Star	Published Lum. class	$\log g$ estimates	Sr/Fe	HRD class pos.	adopted Lum. class
HR 5072	V	3.8-3.9 (IV-V)	IV-V	IV-V	IV-V
HR 4995	IV-V	3.0-3.7 (III/IV)	IV	IV	IV
HR 5409	IV	3.3-3.9 (III/IV)	III-IV	III-IV	III-IV
HR 6608	IIIb	...	IV	IV	IV

NOTE.—Published luminosity classes from Keenan & McNeil (1989). The range of published $\log g$ estimates come from the compilation of Cayrel de Strobel et al. (2001). “Sr/Fe class” is from measuring the $\text{Fe I} \lambda 4071/\text{Sr II} \lambda 4071$ ratio in our spectra and intercomparison to the spectral standards in Table 3 (see Fig. 1). The luminosity class from the HRD position uses the V and $B - V$ data from it Hipparcos and the standard relations from Appendix B of Gray (1991).